SEMI BLIND TIME DOMAIN EQUALIZATION FOR MIMO – OFDM SYSTEMS

A THESIS SUBMITTED IN PARTIAL FULFILMENT OF THE REQUIRMENTS FOR THE DEGREE OF

Master of Technology

In

Telematics and Signal Processing

By

GAMIDI VENKATA RAJESH

Roll No: 207EC101

Department of Electronics & Communication Engineering

National Institute of Technology, Rourkela

May 2009

SEMI BLIND TIME DOMAIN EQUALIZATION FOR MIMO – OFDM SYSTEMS

A THESIS SUBMITTED IN PARTIAL FULFILMENT OF THE REQUIRMENTS FOR THE DEGREE OF

Master of Technology
In
Telematics and Signal Processing

By

GAMIDI VENKATA RAJESH

Roll No: 207EC101

Under the Guidance of

Prof. SARAT KUMAR PATRA

Department of Electronics & Communication Engineering

National Institute of Technology, Rourkela

May 2009

Dept. of Electronics & Communication Engineering
National Institute of Technology
Rourkela-769008

C E R T I F I C A T E

This is to certify that the thesis entitled, **"SEMI BLIND TIME DOMAIN EQUALIZATION FOR MIMO – OFDM SYSTEMS"** submitted by Mr. **GAMIDI VENKATA RAJESH (207EC101** in partial fulfillment of the requirements for the award of Master of Technology Degree in **ELECTRONICS & COMMUNICATION ENGINEERING** with specialization in **"TELEMATICS and SIGNAL PROCESSING"** at the National Institute of Technology, Rourkela is an authentic work carried out by him under my supervision and guidance.

To the best of my knowledge, the matter embodied in the thesis has not been submitted to any other University / Institute for the award of any Degree or Diploma.

Date**:**

Prof. SARAT KUMAR PATRA
(Supervisor)
HOD, Dept. of E&CE
National Institute of Technology
ROURKELA

ACKNOWLEDGEMENTS

This project is by far the most significant accomplishment in my life and it would be impossible without people who supported me and believed in me.

I would like to extend my gratitude and my sincere thanks to my honorable, esteemed supervisor **Prof. Sarat Kumar Patra,** head, Department of Electronics & Communication Engineering. He is not only a great lecturer with deep vision but also most importantly a kind person. I sincerely thank for his exemplary guidance and encouragement. His trust and support inspired me in the most important moments of making right decisions and I am glad to work under his supervision.

I would like to express my humble respects to **Prof. G. S. Rath, Prof. G. Panda, Prof. K. K. Mahapatra, Prof. S. Meher** and **Prof. S. K. Behera** for teaching me and also helping me how to learn. They have been great sources of inspiration to me and I thank them from the bottom of my heart.

I would like to thank all my friends and especially my classmates for all the thoughtful and mind stimulating discussions we had, which prompted us to think beyond the obvious. I've enjoyed their companionship so much during my stay at NIT, Rourkela.

I would like to thank all those who made my stay in Rourkela an unforgettable and rewarding experience.

Last but not least I would like to thank my parents, who taught me the value of hard work by their own example. They rendered me enormous support being apart during the whole tenure of my stay in NIT Rourkela.

(GAMIDI VENKATA RAJESH)

CONTENTS

ABSTRACT

Since the available frequency spectrum is scare, the future systems which relay on broadband applications such as high-speed wireless computer networks should be characterized by significantly enhanced spectral efficiency in order to increase the speed of operation and network capacity. A very promising approach is to use multiple antennas at both the transmitter and receiver (i.e. a Multi-Input Multi-Output (MIMO) system). With such a system the throughput can be increased by simultaneously transmitting different streams of data on the different transmit antennas. Although these parallel data streams are mixed up in the air, they can be recovered at the receiver using multiple receive antennas.

The problem with most of the wireless communication systems now-a-days is multi-path fading effects. Frequency Division multiplexing (FDM) is one of the possible solutions, where the available fading channel bandwidth is partitioned into multiple flat narrow band channels. Orthogonal Frequency Division Multiplexing (OFDM) has become a popular modulation method in high speed wireless communications. By providing orthogonality between the flat narrowband channels, OFDM is able to mitigate the effects of multi-path fading using an equalizer. In a typical OFDM broadband wireless communication system, a guard interval is inserted to avoid the inter-symbol interference (ISI) and the inter-carrier interference (ICI). This guard interval is required to be at least equal to the maximum channel delay spread. Otherwise equalization is required at the receiver.

In this thesis, a semi-blind time-domain equalization technique is proposed for general MIMO OFDM systems. The received OFDM symbols are shifted by more than or equal to the cyclic prefix (CP) length, and a blind equalizer is designed to completely suppress both inter-carrier interference (ICI) and inter-symbol interference (ISI) using second-order statistics of the shifted received OFDM symbols. Only a one-tap equalizer is needed to detect the time domain signals from the blind equalizer output, and one pilot OFDM symbol is utilized to estimate the required channel state information for the design of the one-tap equalizer. Simulation results show that this technique is robust against the number of shifts in excess of the CP length.

LIST OF FIGURES

Figure No. Page No.

LIST OF TABLES

NOMENCLATURE

Abbreviations

ACF	Auto Correlation Function
ADSL	Asymmetric Digital subscriber Line
AWGN	Additive White Gaussian Noise
BER	Bit Error Rate
BPSK	Binary Phase Shift Keying
BSI	Blind System Identification
CP	Cyclic Prefix
CDMA	Code Division Multiple Access
DAB	Digital Audio Broadcast
DFT	Discrete Fourier Transform
DMT	Discrete Multi-Tone
DSPr	Digital Signal Processer
DVB	Digital Video Broadcast
ETSI	European Telecommunications Standards Institute
FDM	Frequency Division Multiplexing
FDE	Frequency Domain Equalizer
FDMA	Frequency Division Multiple Access
FFT	Fast Fourier Transform
FIR	Finite Impulse Response
HOS	Higher Order Statistics
IBI	Inter Block Interference
ICI	Inter Carrier Interference
IDFT	Inverse Discrete Fourier Transform
IFFT	Inverse Fast Fourier Transform
IIR	Infinite Impulse Response

ISI	Inter Symbol Interference
LTI	Linear Time Invariant
MAI	Multiple Access Interference
MCM	Multi carrier Modulation
MIMO	Multi Input Multi Output
ML	Maximum Likelihood
MMSE	Minimum Mean Squared Error
OFDM	Orthogonal Frequency Division Multiplexing
P/S	Parallel to Serial
QAM	Quadrature Amplitude Modulation
QPSK	Quadrature Phase Shift Keying
RF	Radio Frequency
SCs	Single carrier system
SISO	Single Input Single Output
SNR	Signal to Noise Ratio
SOS	Second Order Statistics
S/P	Serial to Parallel
TDE	Time Domain Equalizer
TEQ	Time Domain Equalization
TDMA	Time Division Multiple Access
WLAN	wireless Local Area Network
ZF	Zero Forcing
ZP	Zero Padding

Greek symbols

Ψ	An arbitrary periodic time domain function
Ω	Angular frequency
σ^2	Noise variance

English symbols

K	No. of excess shifts in received symbols
L	Channel length
M	No. of Transmitting antennas in MIMO-OFDM
N	No. of orthogonal sub-carriers
P	No. of Receiving antennas in MIMO-OFDM
T	Time period of a symbol
j	square root of '-1'; (complex number)
Δf	Sub-carrier spacing
u[n]	Source signal
w[n]	Vector representing the Noise sequence at time n
x[n]	Vector representing the Input sequence at time n
y[n]	Vector representing the Output sequence at time n
$A_c(t)$	Amplitude of the carrier
$\omega_c(t)$	Frequency of the carrier
$\Phi_c(t)$	Phase of the carrier
F_N	An NxN DFT matrix
H_{ij}	Channel coefficient's matrix
L_{CP}	Cyclic Prefix length
N'	length of an OFDM symbol after CP insertion
$S_c(t)$	Carrier signal
s_{ip}	i^{th} block OFDM symbol from p^{th} transmitting antenna
T_{FFT}	FFT period in samples
T_G	Length of Guard period in samples
T_S	Length of symbol after CP insertion in samples
$X[k]$	DFT of x[n] sequence

Operators

$[\ ]^*$	Conjugate of a sequence/Conjugate transpose of a matrix
$[\ ] * [\ ]$	Linear Convolution
$[\ ] \otimes [\ ]$	Circular Convolution
$[\ ]^T$	Transpose of a matrix
$[\ ]^{-1}$	Inverse of a matrix
$[\ ]^H$	Pseudo inverse of a matrix
$\|\ \|$	Absolute value
$E\{\ \}$	Estimation of a sequence
$F\{\ \}$	Fourier Transform of a sequence
$R(\ )$	Auto Correlation Function of a sequence

CHAPTER- 1

INTRODUCTION

1.1 Introduction to Frequency Division Multiplexing

In a basic communication system, the data are modulated onto a single carrier frequency. The available bandwidth is then totally occupied by each symbol. This kind of system can lead to inter-symbol-interference (ISI) in case of frequency selective channel. The basic idea of OFDM is to divide the available spectrum into several orthogonal subchannels so that each narrowband subchannel experiences almost flat fading. Orthogonal frequency division multiplexing (OFDM) is becoming the chosen modulation technique for wireless communications. OFDM can provide large data rates with sufficient robustness to radio channel impairments. In an OFDM scheme, a large number of orthogonal, overlapping, narrow band sub-carriers are transmitted in parallel. These sub-carriers divide the available transmission bandwidth. The separation of the sub-carriers is such that the efficiency of spectral utilization is high. With OFDM, it is possible to have overlapping subchannels in the frequency domain, thus increasing the transmission rate. The use of FFT technique to implement modulation and demodulation functions makes it computationally more efficient.

The attractive feature of OFDM is the way it handles the multipath interference at the receiver. Multipath phenomenon generates two effects (a) Frequency selective fading and (b) Intersymbol interference (ISI). The "flatness" perceived by a narrowband channel overcomes the frequency selective fading. On the other hand, modulating symbols at a very low rate makes the symbols much longer than channel impulse response and hence reduces the ISI. Insertion of an extra guard interval between consecutive OFDM symbols can reduce the effects of ISI even more but leads to low system capacity. To achieve high system capacity for multimedia applications in wireless communications, various methods have been proposed in recent years. Among them, the multiple input– multiple output (MIMO) system using multiple antennas at both the transmitter and the receiver has attracted a lot of research interest due to its potential to increase the system capacity without extra bandwidth [1].

To combat the effect of frequency selective fading, MIMO is generally combined with orthogonal frequency-division multiplexing (OFDM) technique, which transforms the frequency-selective fading channels into parallel flat fading subchannels, as long as the cyclic prefix (CP) inserted at the beginning of each OFDM symbol is longer than or equal to the channel length [2]. In this case, the signals on each subcarrier can be easily detected by a one-tap frequency domain equalizer (FDE). In cases where a short CP is inserted for increasing bandwidth efficiency, or because of some unforeseen channel behavior, the effect of frequency-selective fading cannot be completely eliminated, and intercarrier interference (ICI) and intersymbol interference (ISI) will be introduced. In this case, the signals on each subcarrier can be easily detected by a one-tap time domain equalizer (TDE). Equalization techniques are thus important in MIMO-OFDM systems.

1.2 Motivation

The radio environment is harsh, due to the many reflected waves (multi path propagation) and other effects. Use of adaptive equalization techniques at the receiver could be a solution, but there are practical difficulties in operating this equalization in real-time at several Mbps with compact, low-cost hardware. A promising candidate that eliminates a need for the complex equalizers is the Orthogonal Frequency Division Multiplexing (OFDM), a multiple carrier modulation technique. OFDM is robust in adverse channel conditions and allows a high level of spectral efficiency. The OFDM waveform can be easily modified to adjust to the delay spread of the channel. OFDM can handle large delay spreads easier to do the independence of the carriers and the flexibility of varying the cyclic prefix length.

Multiple access techniques which are quite developed for the single carrier modulations (e.g. TDMA, FDMA) have made it possible to share a single communication medium by multiple numbers of users simultaneously. The sharing is required to achieve high capacity by simultaneously allocating the available bandwidth to multiple users without severe degradation in the performance of the system [3]. FDMA and TDMA are the well known multiplexing techniques used in wireless communication systems. While working with the wireless systems using these techniques various problems encountered are (1) multi-path fading (2) time dispersion which lead ISI (3) lower bit rate capacity (4) requirement of larger transmit power for high bit rate and (5) less spectral efficiency.

Disadvantage of FDMA technique is its bad spectrum usage. Disadvantage of TDMA technique is multi-path delay spreading problem. In a typical terrestrial broadcasting, the transmitted signal arrives at the receiver using various paths of different path lengths. Since multiple versions of the signal interfere with each other, it becomes difficult to extract the original information. The orthogonal frequency division multiplexing (OFDM) provides better solution for the above mentioned problems by using MIMO technique.

1.3 Literature Survey

In the classical parallel data system, the total signal frequency band is divided into N non-overlapping frequency subchannels. Each subchannel is modulated with a separate symbol and then the N subchannels are frequency-multiplexed. It seems good to avoid spectral overlap of channels to eliminate interchannel interference (ICI). However, this leads to inefficient use of the available spectrum. To cope with the inefficiency, the idea proposed from the mid-1960s was to use parallel data and FDM with overlapping subchannels, where each subchannel carries a signaling rate 'b' bps, spaced 'b' Hz apart in frequency to avoid the use of high-speed equalization and to combat impulsive noise and multipath distortion, as well as to fully use the available bandwidth. This takes advantage of frequency null of all frequencies except the desired one.

In a single-carrier system, a single fade or interferer can cause the entire link to fail, but in a multicarrier system, only a small percentage of the single carrier system (SCs) will be affected. Error-correction coding can then be used to correct for the few erroneous SCs [4]. Figure 1.1 illustrates the difference between the conventional non overlapping multicarrier technique and the overlapping multicarrier modulation technique. By using the overlapping multicarrier modulation technique, we can save almost 50% of bandwidth. To realize this technique, however, we need to reduce cross talk between SCs, which means that we require orthogonality between different modulated carriers.

The concept of using parallel data transmission by means of frequency division multiplexing (FDM) was reported in mid 60s [5, 6]. Some early developments were happened in the 50s. A patent was filled and issued in January 1970. The idea was to use parallel data streams and FDM with overlapping sub channels to avoid the use of high-speed equalization and to combat impulsive noise, multipath distortion as well as to use the entire available bandwidth. The initial applications were in the military communications. In the telecommunications field, the terms of discrete multi-tone (DMT), multichannel modulation and multicarrier modulation (MCM) are widely used and sometimes they are interchangeable with OFDM. In OFDM, each carrier is orthogonal to all other carriers. However, this condition is not always maintained in MCM [7].

Orthogonal Frequency Division Multiplexing (OFDM) is an alternative wireless modulation technology to CDMA. OFDM has the potential to surpass the capacity of CDMA systems and provide the wireless access method for 4G systems. OFDM is a modulation scheme that allows digital data to be efficiently and reliably transmitted over a radio channel, even in multipath environments.

OFDM is an optimal version of multicarrier transmission schemes. In 1971 Weinstein and Ebert [8] demonstrated the use of discrete Fourier transform (DFT) [9] to parallel data transmission system as part of the modulation and demodulation process. In the 1980s, OFDM has been ideally applied for high speed modems, digital mobile communications [10] and high-density recording.

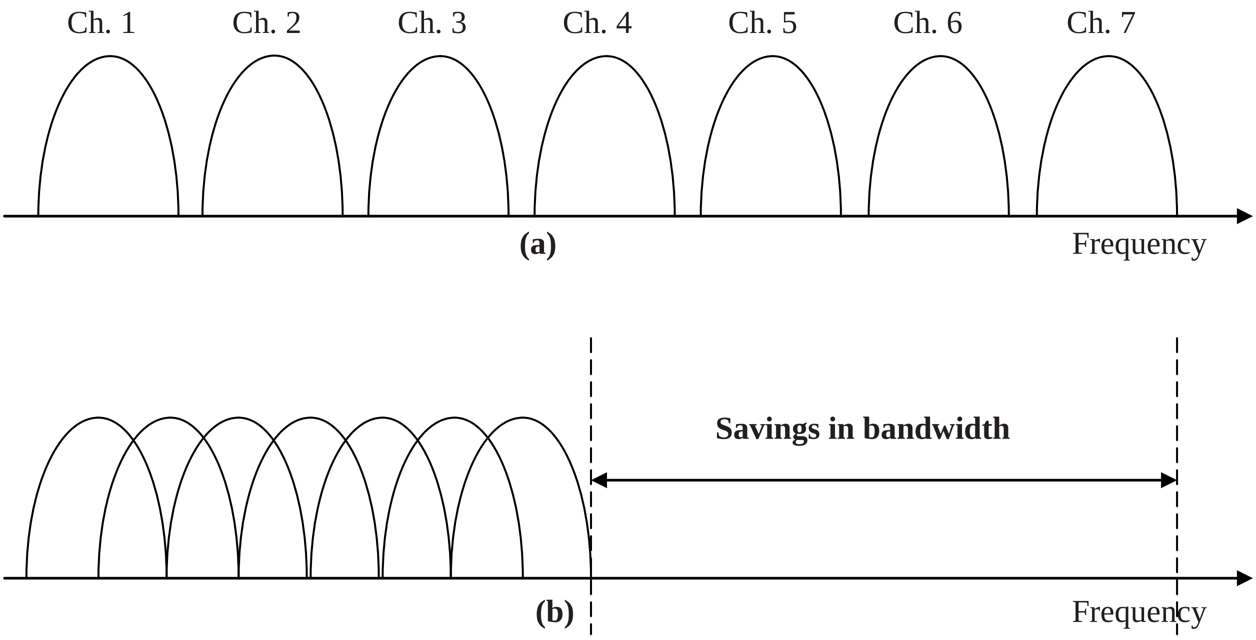

Figure 1.1: Concept of the OFDM signal: (a) conventional multicarrier technique, and (b) orthogonal multicarrier modulation technique.

Various fast modems have been developed for telephone networks. In the 1990s, OFDM has been exploited for wideband data communications over mobile radio FM channels [11], wireless LAN (WLAN) [12], wireless multimedia communication, asymmetric digital subscriber lines (ADSL) [13], very high speed digital subscriber lines (VHDSL), digital audio broadcasting (DAB) and HDTV terrestrial broadcasting[14]. A brief history of OFDM technique and its applications are listed in Table 1.1. In the past few years, application of OFDM technique in WLAN approach has received a considerable attention. This technique has been adopted in the WLAN standards of IEEE 802.11a in North America and HIPERLAN/2 in Europe. It has also been used for the IEEE 802.11g and the IEEE 802.16 WLAN standards.

1957	Kineplex, multi-carrier high frequency (HF) modem
1966	R. W. Chang, Bell Labs, OFDM paper patent
1971	Weinstein & Ebert proposed the use of FFT and guard interval
1985	Cimini described the use of OFDM for mobile communications
1995	ETSI established the first OFDM based standard, digital audio broadcasting (DAB) standard
1997	Broadband internet with asymmetrical digital subscriber line (ADSL) was employed
1998	Magic WAND project demonstrated OFDM modems for wireless LAN
1999	IEEE 802.11a and HIPERLAN/2 standards were established for WLAN
2000	Vector OFDM (V-OFDM) for a fixed wireless access
2001	OFDM was considered for the IEEE 802.11g and the IEEE 802.16 standards

Table 1.1 History of OFDM technique and its applications

1.4 Contribution of Thesis

Using MATLAB, simulation of MIMO-OFDM is done with different modulation techniques using DFT and IDFT techniques. The digital modulation schemes such as BPSK and QPSK were selected to assess the performance of the designed OFDM system by finding their bit error rate (BER) for different values of signal to noise ratio (SNR).

A blind equalizer is designed to completely suppress both inter-carrier interference (ICI) and inter-symbol interference (ISI) using second-order statistics (SOS) of the shifted received OFDM symbols**.** This technique is applied with different number of shifts in the received symbols. The whole simulation is done for both the cyclic prefix (CP) and zero padding (ZP) techniques by varying the length of CP added and compared their Bit error rate (BER) performance.

1.5 Thesis Organization

Following the introduction, the rest of the thesis is organized as follows. Chapter 2 gives an overview of OFDM. It describes OFDM basic principle, its working model, properties, parameters, and applications. Chapter 3 describes the multipath environment, MIMO techniques and application of MIMO to OFDM i.e. MIMO-OFDM. Chapter 4 describes different equalization techniques used in wireless communication systems. Chapter 5 describes OFDM simulations and results using semi-blind time domain equalization technique. Then the conclusion to my work and the points to possible directions for future work are given in further sessions. References are included at the end of this thesis.

CHAPTER- 2

An Introduction to OFDM

2.1 Introduction

A sinusoidal wave behaves as an eigen function for a linear time invariant (LTI) system and is less susceptible to interference. Hence a sine wave is suitable for transmission on a multi-tap channel. The sine waves used for transmission should be over sufficiently long intervals of time in order to preserve the eigen property. Therefore distinct multiple sinusoids of sufficient duration modulated by data symbols can be used to transmit data with a lesser degradation in performance. However, adjacent sub-carriers in frequency should be separated by guard bands to prevent overlap of information between them resulting in poor bandwidth efficiency.

2.2 Orthogonality of signals

The main concept in OFDM is Orthogonality of the sub-carriers. Since the carriers are all either sin or cosine waves, we know that the area under the sine wave or cosine wave is zero as shown in Figure 2.1.

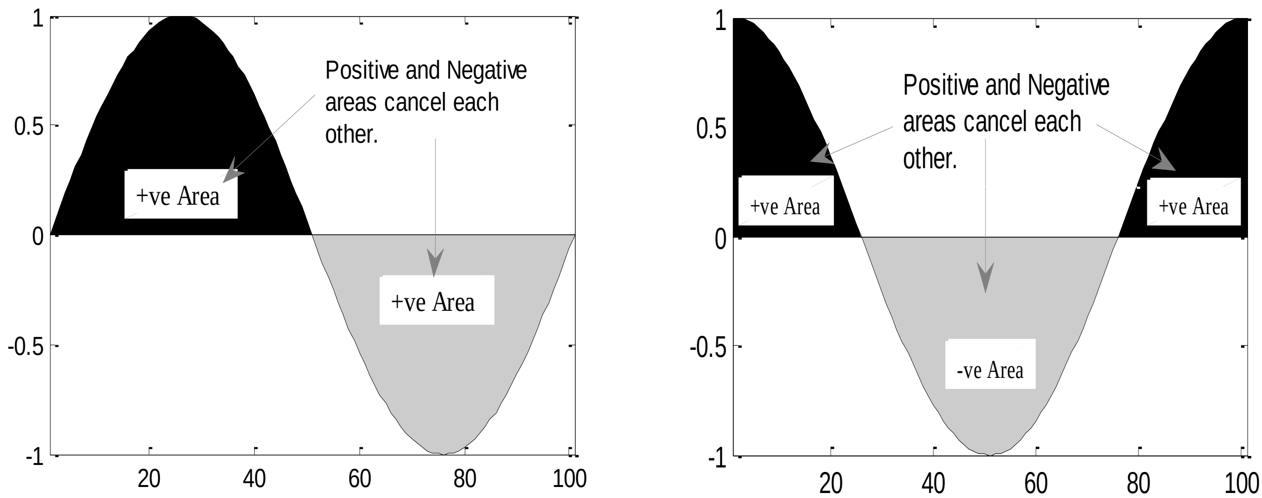

Figure 2.1: The area under a sine and a cosine wave over one period.

Let's take a sine wave of frequency *m* and multiply it by a sinusoid (sine or cosine) of a frequency *n*, where both *m* and *n* are integers. The integral or the area under this product is given by

$$f(t) = \sin(mwt) * \sin(nwt) \quad (2.2.1)$$

By the simple trigonometric relationship, the equation 2.2.1 is equal to sum of two sinusoids *(n-m)* and *(n+m)*, if $n>m$

$$=\frac{1}{2}\cos(n-m)-\frac{1}{2}\cos(n+m) \qquad (2.2.2)$$

Again these two components are sinusoids each, so the integral over one period is zero.

$$=\int_0^{2\pi}\frac{1}{2}\cos((n-m)t)dt-\int_0^{2\pi}\frac{1}{2}\cos((n+m)t)dt \qquad (2.2.3)$$

$= 0 – 0 = 0.$

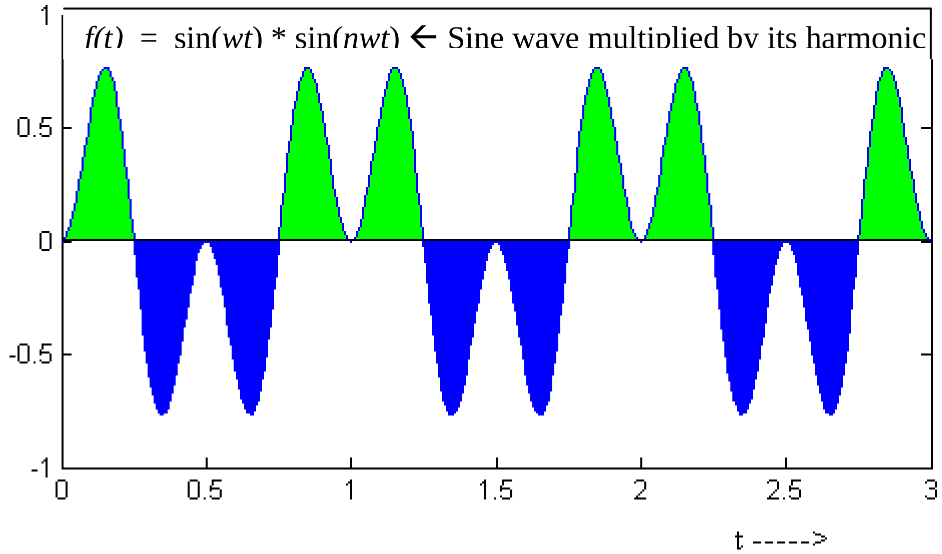

Figure 2.2: The area under a sine wave multiplied by its own harmonic is zero always

It can be concluded that when a sinusoid of frequency *n* is multiplied by a sinusoid of frequency *m/n*, the area under the product is zero. This is shown in Figure 2.2. The positive area (gray colored) and the negative area (black colored) are equal in magnitude over one period and hence cancel each other. In general for all integers *m* and *n* the functions sin(*nx*), sin(*mx*), cos(*mx*) and cos(*nx*) are all orthogonal to each other. These frequencies are called “Harmonics”.

This idea is the key to understand the working of OFDM. The orthogonality allows simultaneous transmission on a single large sub-carrier in a tight frequency space without interference from each other. In essence this is similar to Code Division Multiple Access (CDMA), where codes are used to make data sequence independent (also orthogonal); which allows many independent users to transmit in same space successfully [15].

2.3 What is OFDM?

OFDM is simply defined as a form of multi-carrier modulation where the carrier spacing is carefully selected so that each sub carrier is orthogonal to the other sub carriers. Two signals are orthogonal if their dot product is zero. That is, two signals are taken and multiplied together. If their integral over an interval is zero, then two signals are orthogonal in that interval. Orthogonality can be achieved by carefully selecting carrier spacing, such as letting the carrier spacing be equal to the reciprocal of the useful symbol period. As the sub carriers are orthogonal, the spectrum of each carrier has a null at the center frequency of each of the other carriers in the system. This results in no interference between the carriers, allowing them to be spaced as close as theoretically possible. Mathematically, suppose there is a set of signals Ψ and let Ψ_p be the p^{th} element in the set. Then,

$$\int_{a}^{a+T} \psi_p(t)\psi_q^*(t) = \begin{cases} K\_for\_p = q \\ 0\_for\_p \neq q \end{cases} \tag{2.3.1}$$

The signals are orthogonal if the integral value is zero over the interval [a a+T], where T is the symbol period. Since the carriers are orthogonal to each other the nulls of one carrier coincides with the peak of another sub carrier. As a result it is possible to extract the sub carrier of interest.

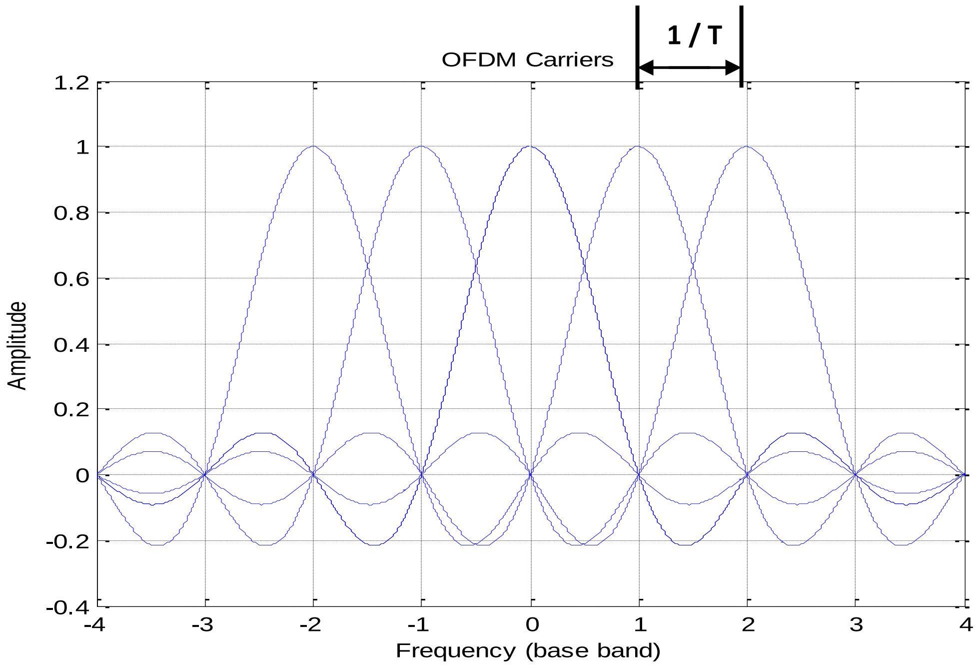

Figure 2.3: Frequency spectrum of OFDM transmission.

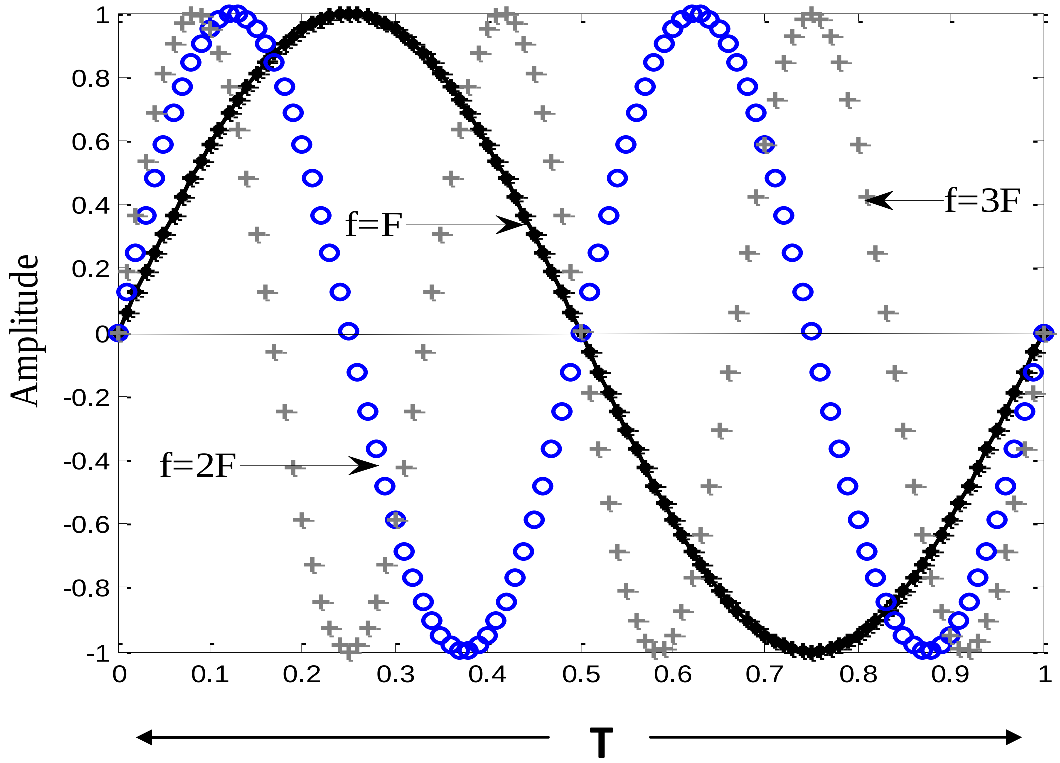

Figure 2.4: Carrier signals in an OFDM transmission

OFDM transmits a large number of narrowband subchannels. The frequency range between carriers is carefully chosen in order to make them orthogonal each another. In fact, the carriers are separated by an interval of 1/T, where T represents the duration of an OFDM symbol. The frequency spectrum of an OFDM transmission is illustrated in Figure 2.3. The Figure indicates the spectrum of carriers significantly over laps over the other carrier. This is contrary to the traditional FDM technique in which a guard band is provided between each carrier. Each 'sinc' of the frequency spectrum in Figure 2.3 corresponds to a sinusoidal carrier modulated by a rectangular waveform representing the information symbol. One could easily notice that the frequency spectrum of one carrier exhibits zero-crossing at central frequencies corresponding to all other carriers. At these frequencies, the intercarrier interference is eliminated, although the individual spectra of subcarriers overlap. It is well known that orthogonal signals can be separated at the receiver by correlation techniques. The receiver acts as a bank of demodulators, translating each carrier down to baseband, the resulting signal then being integrated over a symbol period to recover the data. If the other carriers beat down to frequencies which, in the time domain means an integer number of cycles per symbol period (T), then the integration process results in a zero contribution from all these carriers [16]. The waveforms of some of the carriers in an OFDM transmission are illustrated in Figure 2.4.

From the Figures illustrated, it is clear that OFDM is a highly efficient system and hence is often regarded as the optimal version of multi-carrier transmission schemes. The number of sub channels transmitted is fairly arbitrary with certain broad constraints, but in practical systems, sub-channels tend to be extremely numerous and close to each other. For example the number of carriers in 802.11a wireless LAN (WLAN) is 48 while for Digital Video Broadcast (DVB) it is as high as 6000 sub carriers.

It is worth mentioning here that relative to a single carrier Modulation technique (SCM), the OFDM system provides a better symbol rate for the total available bandwidth. This characteristic is not a problem given that the carriers overlap significantly. The slow $\frac{\sin(x)}{x}$ roll off, which provides a wider carrier bandwidth, is only an issue at the edge of the channel spectrum. Standards like IEEE 802.11a allow the rectangular pulse to be modified such that the rising and falling edges are soften (Raised cosine) at the edge of their assigned spectrum. This helps constrain the spectrum without affecting data transmissions.

2.4 Mathematical Analysis

With an overview of the OFDM system, the mathematical definition of the modulation system is presented here. It is important to know that the carriers generated by the IFFT chip are mutually orthogonal. This is true from the very basic definition of an IFFT signal. This allows understanding how the signal is generated and how receiver must operate. Mathematically, each carrier can be described as a complex wave:

$$S_C(t) = A_C(t) * e^{j(\omega_c(t)+\phi_C(t))} \tag{2.4.1}$$

The real signal is the real part of $S_c(t)$. $A_c(t)$ and $\Phi_c(t)$ are the amplitude and phase of the carrier 'C' and can vary over a symbol by symbol basis. The values of the parameters are constant over the symbol duration period. OFDM consists of many carriers. Thus the complex signal $S_c(t)$ is represented by:

$$S_C(t) = \frac{1}{N}\sum_{n=0}^{N-1} A_n(t) * e^{j(\omega_n(t)+\phi_n(t))} \tag{2.4.2}$$

Where $\omega_n = \omega_0 + n\Delta\omega$ is the n[th] carrier with ω_0 as the initial carrier and $\Delta\omega$ is the carrier spacing.

This is the case of continuous signal. If the waveform of each component of the signal over one symbol period is considered, then the variables $A_c(t)$ and $\Phi_c(t)$ take on fixed values, which depend on the frequency of that particular carrier, and so can be rewritten as:

$$\phi_C(t) = \phi_C \qquad \text{and} \qquad A_C(t) = A_C \tag{2.4.3}$$

If the signal is sampled using a sampling frequency of 1/T, then the resulting signal is represented by:

$$S_C(kT) = \frac{1}{N}\sum_{n=0}^{N-1} A_n * e^{j((\omega_0 + n\Delta\omega)+\phi_n)} \tag{2.4.4}$$

At this point the signal under analysis is restricted to N samples only. It is convenient to sample over the period of one data symbol. Thus we have a relationship: t=NT. By simplifying equation (2.4.4), without a loss of generality by letting ω_0=0, the signal can be represented as:

$$S_C(kT) = \frac{1}{N}\sum_{n=0}^{N-1} A_n * e^{j\phi_n} e^{j(n\Delta\omega)kT} \tag{2.4.5}$$

Now equation (2.4.5) can be compared with the general form of the inverse Fourier transform

$$g(kT) = \frac{1}{N}\sum_{n=0}^{N-1} G\left(\frac{n}{NT}\right) e^{\frac{2\Pi}{N}kn} \tag{2.4.6}$$

In equation (2.4.5) the function "A_n $e^{j\Phi n}$ " is no more than a definition of the signal in the sampled frequency domain, and $S_c(kT)$ is the time domain representation.

Equations 2.4.6 and 2.4.7 are equivalent if and only if:

$$\Delta f = \frac{\Delta\omega}{2\Pi} = \frac{1}{NT} = \frac{1}{\tau}, \ \tau \text{ is a constant.} \tag{2.4.7}$$

This is the same condition that was required for orthogonality Thus, one consequence of maintaining orthogonality is that the OFDM signal can be defined by using Fourier transform procedures.

2.5 Principles of OFDM

In a conventional serial data system, the symbols are transmitted sequentially, one by one, with the frequency spectrum of each data symbol allowed to occupy the entire available bandwidth. A high rate data transmission supposes very short symbol duration, conducing at a large spectrum of the modulation symbol. There are good chances that the frequency selective channel response affects in a very distinctive manner the different spectral components of the data symbol, hence introducing the ISI [17].

The same phenomenon, regarded in the time domain consists in smearing and spreading of information symbols such, the energy from one symbol interfering with the energy of the next ones, in such a way that the received signal has a high probability of being incorrectly interpreted. Intuitively, one can assume that the frequency selectivity of the channel can be mitigated if, instead of transmitting a single high rate wide band data stream, we can transmit the data simultaneously on several narrow-band subchannels (with a different carrier corresponding to each sub-channels). This provides a flat frequency response for each channel. This is represented in Figure 2.5.

Hence, for a given data rate, increasing the number of carriers reduces the data rate that each individual carrier can provide, therefore lengthening the symbol duration on each subcarrier. Slow data rate on each subchannel merely means that the effects of ISI are severely reduced. This is the basic idea that lies behind OFDM.

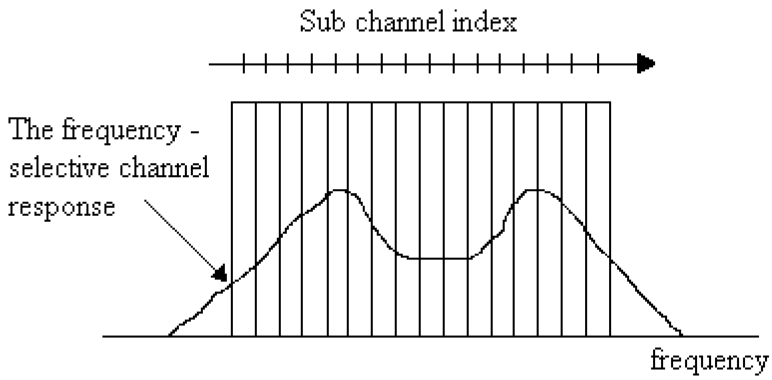

Figure 2.5: The frequency selective channel response and relatively flat response on each sub channel

Transmitting the data among a large number of closely spaced subcarriers accounts for the “frequency division multiplexing” (FDM), the second part of the name OFDM. Unlike the classical FDM technique, OFDM will provide much higher bandwidth efficiency as shown in Figure 1.1. This is due to the fact that in OFDM the spectra of individual subcarriers are allowed to overlap. In fact, the carriers are carefully chosen to be orthogonal each other. It is well known that the orthogonal signals do not interfere and they can be separated at the receiver by correlation techniques. Orthogonality of the subcarriers accounts for the first part of the OFDM name.

2.5.1 OFDM system block diagram

Figure 2.6 presents a classical OFDM transmission scheme that uses Fast Fourier Transform (FFT). The input data sequence is baseband modulated, using a digital modulation scheme. Various modulation schemes could be employed such as BPSK, QPSK (also with their differential form) and QAM with several different signal constellations. There are also forms of OFDM where a distinct modulation on each subchannel is performed (e.g. transmitting more bits using an adequate modulation method on the carriers that are more “confident”, like in ADSL systems). The modulation is performed on each parallel sub stream that is on the symbols belonging to adjacent DFT frames. The data symbols are parallelized in N different sub streams. Each sub stream will modulate a separate carrier through the IFFT modulation block, which is the key element of OFDM scheme. A cyclic prefix is inserted in order to eliminate the inter symbol interference (ICI) and inter block interference (IBI) [7].

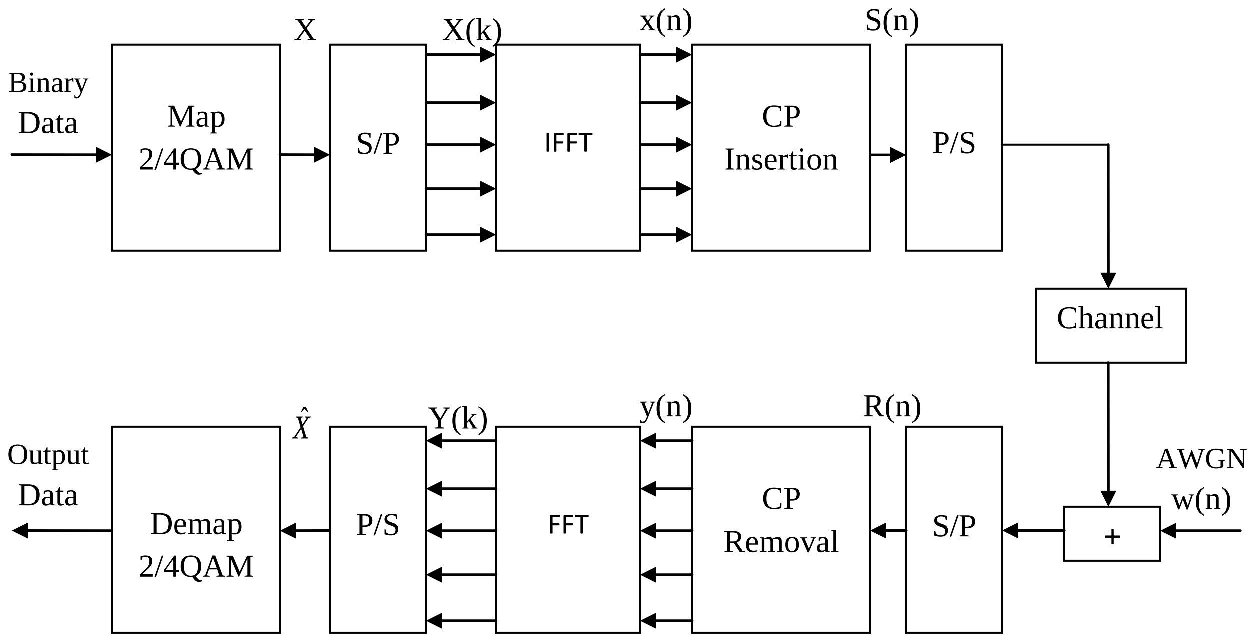

Figure 2.6: The block diagram of an OFDM system

This cyclic prefix of length L is a circular extension of the IFFT-modulated symbol, obtained by copying the last L samples of the symbol in front of it. The data is back-serial converted, forming an OFDM symbol that modulates a high-frequency carrier before transmitting through the channel. The radio channel is generally referred as a linear time variant system. To the receiver, the inverse operations are performed; the data is down converted to the baseband and the cyclic prefix is removed. The coherent FFT demodulator will ideally retrieve the exact form of transmitted symbols. The data is serial converted and the appropriated demodulation scheme is used to estimate the transmitted symbols.

2.5.2 The concept of multicarrier (parallel) transmission

In a mobile radio environment, the signal is carried by a large number of paths with different strength and delays. Such multipath dispersion of the signal is commonly referred as, "channel-induced ISI" and yields the same kind of ISI distortion caused by an electronic filter [17]. In fact, the multipath dispersion leads to an upper limitation of the transmission rate in order to avoid the frequency selectivity of the channel or the need of a complex adaptive equalization in the receiver. In order to mitigate the time-dispersive nature of the channel, the finding of the multicarrier technique replaces a single carrier serial transmission at a high data rate with a number of slower parallel data streams. Each parallel stream is then used to sequentially modulate a different carrier. By creating N parallel sub streams, we will be able to decrease the bandwidth of the modulation symbol by the factor of N, or, in other words, the duration of a modulation symbol is increased by the same factor. The summation of all of the individual subchannel data rates will result in total desired symbol rate, with the drastic reduction of the ISI distortion. The price to pay is of course very important, since the multicarrier transmission seems to be a frequency multiplex technique, which will generate problems in terms of bandwidth efficiency usage. The things go however better than seemed, because in OFDM the carriers are orthogonal to each-other and they are separated by a frequency interval of f =1/T. The frequency spectrum of the adjacent subchannels will overlap one another, but the carrier's orthogonality will eliminate in principle the inter channel interference (ICI).

2.5.3 The Discrete Fourier Transform (DFT)

Though Multi carrier technique was introduced in the 1950 [18], the main reason that hindered the OFDM expansion for a very long time was practical implementation. It was difficult to generate such a signal, and even harder to receive and appropriately demodulate such a signal. Also this technique required a very large array of sinusoidal generators and also a large array of coherent demodulators to make the work. Therefore, the hardware solution can't be practical.

Recent explosive development of digital signal processors (DSPr) has provided breakthrough to the generation and demodulation of an OFDM signal, the magic idea was to use Fast Fourier Transform (FFT), a modern DSP technique. FFT merely represents a rapid mathematical method for computer applications of Discrete Fourier Transform (DFT). In fact, the signal is generated using the Inverse Fast Fourier Transform (IFFT), the fast implementation of Inverse Discrete Fourier Transform (IDFT).

There is a mysterious connection between this transform and the concept of multicarrier modulation. According to its mathematical distribution, IDFT summarizes all sine and cosine waves of amplitudes stored in X[k] array, forming a time domain signal shown below :

$$x(n) = \sum_{k=0}^{N-1} X[k] e^{(\frac{j2\pi nk}{N})}$$

$$= \sum_{k=0}^{N-1} X[k] * \left\{ \cos(\frac{2\pi nk}{N}) + j * \sin(\frac{2\pi nk}{N}) \right\}, n = 0,1,\ldots, N-1 \qquad (2.5.1)$$

From equation (2.5.1), we can simply observe that IDFT takes a series of complex exponential carriers, modulate each of them with a different symbol from the information array X[k], and multiplexes all this to generate N samples of a time domain signal as shown in Figure 2.7**.** In DFT block the reverse operation takes place, where the series of complex exponential carriers with 90^0 phase difference are modulated with a different symbol from the information array x[n], which is in time domain and multiplexes all this to generate N samples of a frequency domain DFT signal .

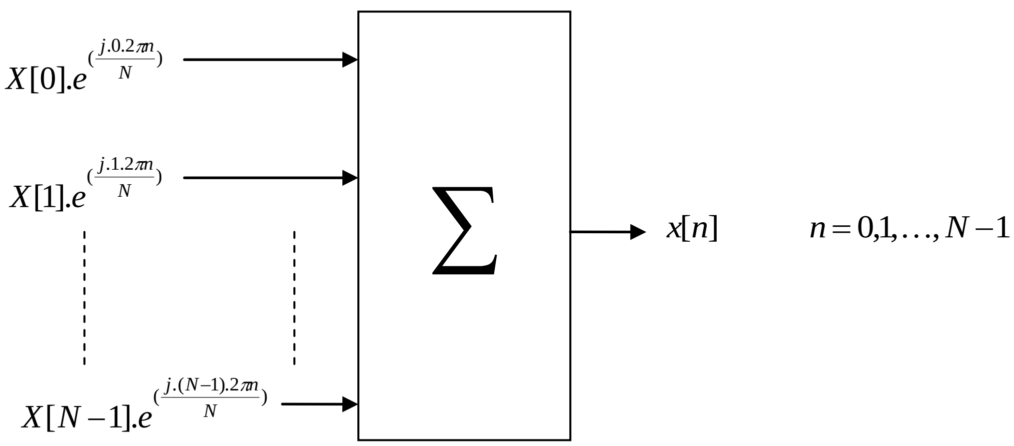

Figure 2.7: IDFT formation using a summer.

The complex exponential carriers are orthogonal to each other, as we know from the Fourier decomposition. These carriers are frequency spaced with $\Delta\Omega = 2\pi/N$. If we consider that the N data symbols X[k] come from sampling an analog information with a frequency of f_s, a way to make discrete to analog frequency conversion indicates a $\Delta f = 1/T$ spacing between the subcarriers of the transmitted signal.

The schema presented in Figure 2.6, relies on a classical signal synthesis algorithm. The N samples of the time domain signal are synthesized from sinusoids and cosinusoids of frequencies $k*2\pi/N$ (The 'weight' with which each complex exponential contributes to the time domain signal). Therefore, the information X[k] to be transmitted could be regarded as being defined in the frequency domain. In its simplest form, when X[k] stores a binary information ('0' or '1'), each symbol to the IDFT entry will simply indicate the presence (a '1') or the absence (a '0') of a certain carrier in the composition of the time domain signal.

At the receiver the inverse process is realized, the time domain signal constitutes the input to a DFT "signal analyzer", implemented of course using the FFT algorithm. The FFT demodulator takes the N time domain transmitted samples and determines the amplitudes and phases of sine and cosine waves, forming the received signal, according to the equation (2.4.2):

$$X(k) = \sum_{k=0}^{N-1} x[n] e^{\left(\frac{-j2\Pi nk}{N}\right)}$$

$$= \sum_{k=0}^{N-1} x[n] * \left\{ \cos\left(\frac{2\pi nk}{N}\right) - j * \sin\left(\frac{2\pi nk}{N}\right) \right\}, k = 0,1,\ldots, N-1 \qquad (2.5.2)$$

2.5.4 The cyclic prefix

For a given system bandwidth the symbol rate for an OFDM signal is much lower than a single carrier transmission scheme. For example for a single carrier BPSK modulation, the symbol rate corresponds to the bit rate of the transmission. However for OFDM the system bandwidth is broken up into N_C sub carriers, resulting in a symbol rate that is N_C times lower than the single carrier transmission. This low symbol rate makes OFDM naturally resistant to effects of Inter-Symbol Interference (ISI) caused by multipath propagation. Multipath propagation is caused by the radio transmission signal reflecting off objects in the propagation environment, such as walls, buildings, mountains, etc.

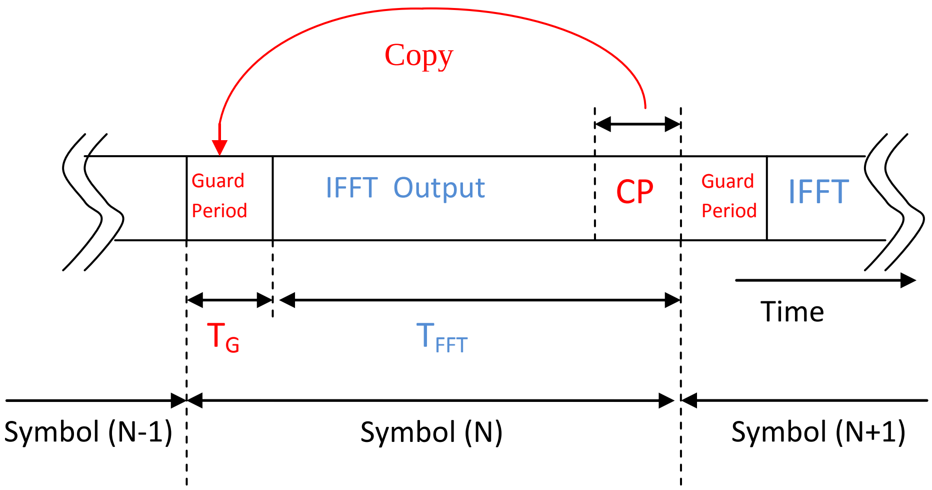

Figure 2.8: Inserting cyclic prefix (CP) to an OFDM symbol

These multiple signals arrive at the receiver at different times due to the transmission distances being different. This spreads the symbol boundaries, causing leakage between them. The effect of ISI on an OFDM signal can be further improved by the addition of a guard period to the start of each symbol. This guard period is a cyclic copy that extends the length of the symbol waveform, known as cyclic prefix (CP). Each sub carrier, in the data section of the symbol, (i.e. the OFDM symbol with no CP added, which is equal to the length of the IFFT size used to generate the signal) has an integer number of cycles. By placing copies of the symbol end-to-end results in a continuous signal with no discontinuities at the joins. Thus by copying the end of a symbol and appending this to the start results in a longer symbol time. Fig 2.8 shows the insertion of a guard period.

The total length of the symbol is $T_S = T_G + T_{FFT}$, where T_S is the total length of the symbol in samples, T_G is the length of the CP in samples and T_{FFT} is the size of the IFFT used to generate the OFDM signal. In addition to protecting the OFDM from ISI, the guard period also provides protection against time-offset errors in the receiver.

2.5.5 Inter-symbol interference

Intersymbol Interference (ISI) is an unavoidable consequence of both wired and wireless communication systems. Morse first noticed it on the transatlantic cables transmitting message using dots and dashes and it has not gone way since. He handled it by just slowing down the transmission [19]. Assume that the time span of the channel is L_C samples long. Instead of a single carrier with a data rate of R symbols/ second, an OFDM system has N subcarriers, each with a data rate of R/N symbols/second. Because the data rate is reduced by a factor of N, the OFDM symbol period is increased by a factor of N. By choosing an appropriate value for N, the length of the OFDM symbol becomes longer than the time span of the channel. Because of this configuration, the effect of intersymbol interference is the distortion of the first L_c samples of the received OFDM symbol[20]. An example of this effect is shown in Figure 2.9.

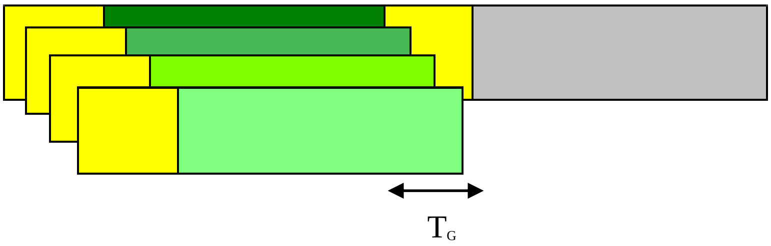

Figure 2.9: Example of inter-symbol interference. The green symbol was transmitted first, followed by the gray symbol.

By noting that only the first few samples of the symbol are distorted, one can consider the use of a guard interval to remove the effect of intersymbol interference [3]. The guard interval could be a section of all zero samples transmitted in front of each OFDM symbol since it does not contain any useful information, the guard interval would be discarded at the receiver. If the length of the guard interval is properly chosen such that it is longer than the time span of the channel, the OFDM symbol itself will not be distorted. Thus, by discarding the guard interval, the effects of intersymbol interference are thrown away as well.

2.6 Advantages and Disadvantages of OFDM

2.6.1 Advantages

The advantages using OFDM are listed below.

- Makes efficient use of the spectrum by allowing overlap.
- By dividing the channel into narrowband flat fading sub channels, OFDM is more resistant to frequency selective fading than single carrier systems.
- OFDM is an efficient way to deal with multipath; for a given delay spread, the implementation complexity is significantly lower than that of a single-carrier system with an equalizer.
- Eliminates ISI and ICI through use of a cyclic prefix.
- Using adequate channel coding and interleaving one can recover symbols lost due to the frequency selectivity of the channel.
- Channel equalization becomes simpler than by using adaptive equalization techniques with single carrier systems.
- It is possible to use maximum likelihood decoding with reasonable complexity.

- OFDM is computationally efficient by using FFT techniques to implement the modulation and demodulation functions.
- It is less sensitive to sample timing offsets than single carrier systems are.
- Provides good protection against co-channel interference and impulsive parasitic noise.

2.6.2 Disadvantages

The disadvantages of OFDM are as follows:

- OFDM has a relatively large peak-to-average-power ratio, which tends to reduce the power efficiency of the radio frequency (RF) amplifier.
- The OFDM signal has a noise like amplitude with a very large dynamic range; therefore it requires RF power amplifiers with a high peak to average power ratio.
- It is more sensitive to carrier frequency offset and drift than single carrier systems are due to leakage of the DFT (Refer Figure 2.10).
- Adding a guard period lowers the symbol rate and hence lowers the overall spectral efficiency of the system.

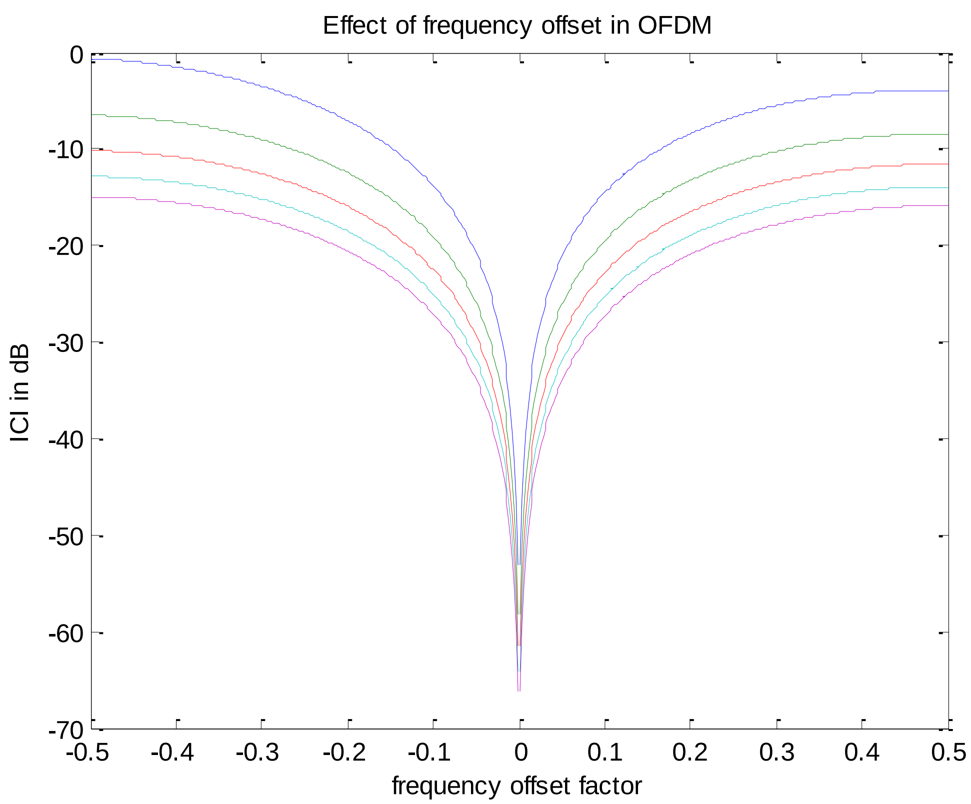

Figure 2.10: Effect of frequency offset in OFDM. The figure shows ICI of one carrier with other orthogonal carriers as a function of offset factor.

The impact of a frequency error can be seen as an error in the frequency instants, where the received signal is sampled during demodulation by the FFT. Figure 2.11 depicts this twofold effect. The amplitude of the desired sub-channel is reduced (indicated by a “+” sign), and ICI arises from the adjacent sub-channels (indicated by an “O” sign).

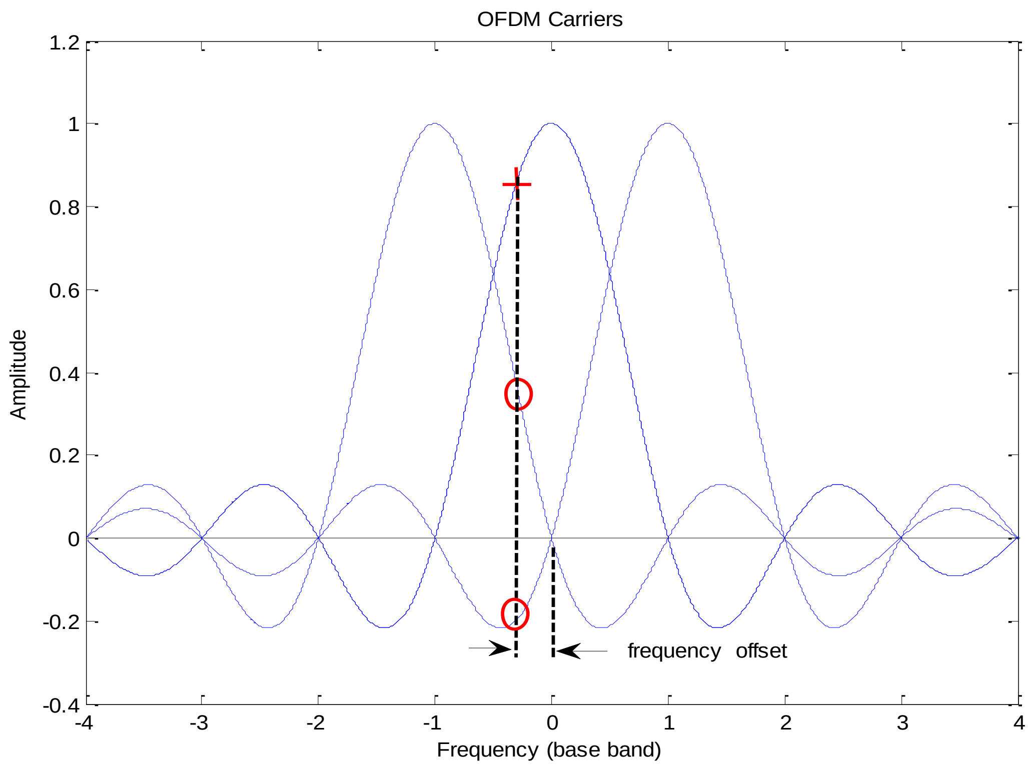

Figure 2.11: Introduction of ICI in the case of a carrier synchronization error.

2.7 Applications of OFDM

- DAB - OFDM forms the basis for the Digital Audio Broadcasting (DAB) standard in the European market.
- ADSL - OFDM forms the basis for the global ADSL (asymmetric digital subscriber line) standard.
- Wireless Local Area Networks - development is ongoing for wireless point-to-point and point-to-multipoint configurations using OFDM technology.
- In a supplement to the IEEE 802.11 standard, the IEEE 802.11 working group published IEEE 802.11a, which outlines the use of OFDM in the 5GHz band.

CHAPTER- 3

An Introduction to MIMO OFDM

3.1 Need for MIMO

The growing demand of multimedia services and the growth of Internet related contents lead to increasing interest to high speed communications. The requirement for wide bandwidth and flexibility imposes the use of efficient transmission methods that would fit to the characteristics of wideband channels especially in wireless environment where the channel is very challenging. In wireless environment the signal is propagating from the transmitter to the receiver along number of different paths, collectively referred as multipath. While propagating the signal power drops of due to the following effects: path loss, macroscopic fading and microscopic fading. Fading of the signal can be mitigated by different diversity techniques. To obtain diversity, the signal is transmitted through multiple (ideally) independent fading paths e.g. in time, frequency or space and combined constructively at the receiver [6].

To achieve a high system capacity for multimedia applications in wireless communications, various methods have been proposed in recent years. Among them, the multiple input – multiple output (MIMO) system using multiple antennas at both the transmitter and the receiver has attracted a lot of research interest due to its potential to increase the system capacity without extra bandwidth [21]. Multiple input- multiple-output (MIMO) exploits spatial diversity by having several transmit and receive antennas. Previous work has shown that the system capacity could be linearly increased with the number of antennas when the system is operating over flat fading channels [1, 22]. In real situations, multipath propagation usually occurs and causes the MIMO channels to be frequency selective. To combat the effect of frequency selective fading, MIMO is generally combined with orthogonal frequency-division multiplexing (OFDM) technique.

OFDM transforms the frequency-selective fading channels into parallel flat fading sub channels, as long as the cyclic prefix (CP) inserted at the beginning of each OFDM symbol is longer than or equal to the channel length [2]. The channel length means the length of impulse response of the channel as discrete sequence. The signals on each subcarrier can be easily detected by a time-domain or frequency-domain equalizer. Otherwise the effect of frequency-selective fading cannot be completely eliminated, and inter-carrier interference (ICI) and inter-symbol interference (ISI) will be introduced in the received signal. Equalization techniques that could flexibly detect the signals in both cases are thus important in MIMO-OFDM systems.

3.2 Multipath Environment

In wireless environment, transmitted signal follow several propagation paths. Many of these paths, having reflected from surrounding objects, reach the receiver with different propagation delays. This multipath leads to delay spread, intersymbol interference (ISI), fading and random phase distortion. Figure 3.1 describes this phenomenon. The corresponding channel impulse response is shown in Figure 3.2.

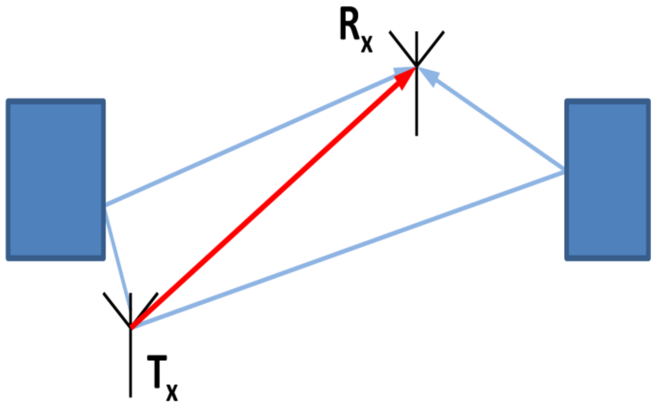

Figure 3.1: Multipath Environment in Wireless Communications

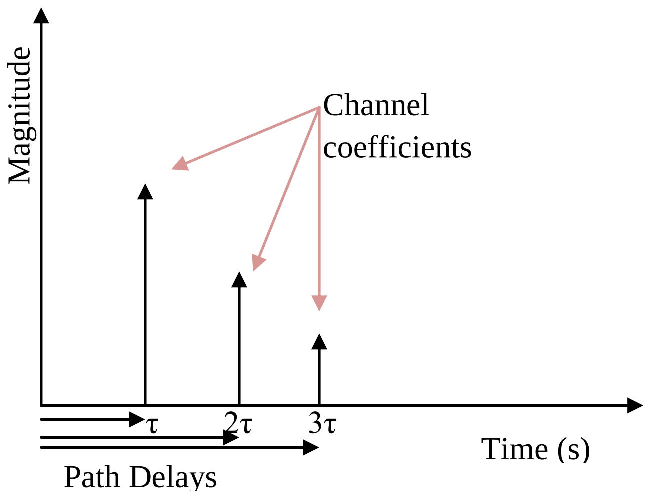

Figure 3.2: Channel Impulse response in Multipath Environment

Delayed copies of the transmitted signal interfere with subsequent signals, causing Inter Symbol Interference (ISI). Therefore transmitted symbol rate is limited by the delay spread of the channel.

Multipath Propagation causes MIMO channels to be frequency selective which cannot have flat frequency response. To combat this effect MIMO is combined with OFDM. OFDM transforms the frequency selective fading channel into parallel flat fading sub channels, but the length of CP inserted should be greater than the channel length.

For a 2 x 2 MIMO-OFDM configuration the received OFDM symbols are given the equations (3.2.1a) & (3.2.1b). The same thing is represented in matrix form in equation (3.2.2). Here the term X_i represents the transmitted symbol from the i^{th} transmitting antenna, the term Y_j represents the received symbol from the j^{th} receiving antenna, the term N_i represents the noise component present in the i^{th} symbol and the term H_{ij} represents the channel coefficient corresponding to the i^{th} transmitting antenna and j^{th} receiving antenna.

Rx. Ant 1: $Y_1(k) = H_{11}(k)X_1(k) + H_{12}(k)X_2(k) + N_1(k)$ (3.2.1a)

Rx. Ant 2: $Y_2(k) = H_{21}(k)X_1(k) + H_{22}(k)X_2(k) + N_2(k)$ (3.2.1b)

$$\begin{pmatrix} Y_1(k) \\ Y_2(k) \end{pmatrix} = \begin{pmatrix} H_{11}(k) & H_{12}(k) \\ H_{21}(k) & H_{22}(k) \end{pmatrix} \begin{pmatrix} X_1(k) \\ X_2(k) \end{pmatrix} + \begin{pmatrix} N_1(k) \\ N_2(k) \end{pmatrix} \qquad (3.2.2)$$

In a Direct path environment, where the reflected waves from multiple objects are absent, the channel looks to be flat and contains a single co-efficient in its impulse response. This type of channel is can be modeled using Additive White Gaussain Noise(AWGN) channel. The model does not account for the phenomena of fading, frequency selectivity, interference, nonlinearity or dispersion. In a multipath environment, the channel is always frequency selective type. This type of channel can be modeled using Rayleigh random distribution.

Figure 3.3 shows simulation results of the Bit error rate(BER) performance of Binary Phase Shift Keying (BPSK) modulation for Rayleigh fading and AWGN channel. The simulation carried out with 10^6 transmitted data bits with random channel coefficients and repeated for experiments.

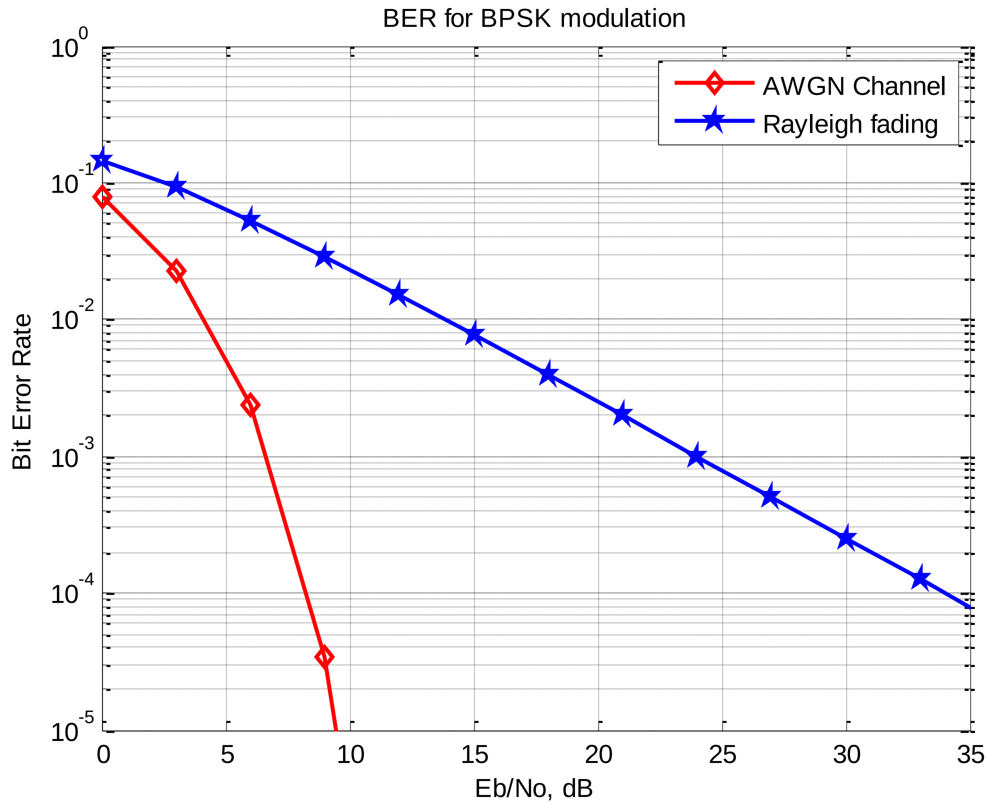

Figure 3.3: Comparison of BER performance for BPSK modulation in AWGN channel and Rayleigh fading channel.

3.3 MIMO channel Configuration

MIMO configuration uses multi-element antenna arrays at both transmitter and receiver, which effectively exploits the third (spatial) dimension in addition to time and frequency dimensions. This architecture achieves channel capacity far beyond that of traditional techniques. In independent Rayleigh channels the MIMO capacity scales linearly as the number of antennas under some conditions. However, some impairments of the radio propagation channel may lead to a substantial degradation in MIMO performance. Some limitations on the MIMO capacity are imposed by the number of multipath components or scatterers [23]. Another limitation on the MIMO channel capacity is due to the correlation between individual sub-channels of the matrix channel [24]. Increase in the correlation coefficient results in capacity decrease and, finally, when the correlation coefficient equals to unity, no advantage is provided by the MIMO architecture [24].

For fixed linear matrix channel with additive white Gaussian noise and when the transmitted signal vector is composed of statistically independent equal power components each with a Gaussian distribution and the receiver knows the channel, its capacity is [25]

$$C = \log_2(\det(I_N + \frac{\rho}{N} H * H^H)) \quad \text{bits/s/Hz} \tag{3.3.1}$$

where 'N' is the number of transmit/receive antennas (for the sake of simplicity, consider the number of transmit and receive antennas are equal); 'ρ' is the average SNR; 'I_N' is an identity matrix of size NxN and 'H' is the normalized channel matrix, which is considered to be frequency independent over the signal bandwidth. The normalization condition used is:

$$\sum_{i,j=1}^{N} \left|h_{ij}\right|^2 = N \tag{3.3.2}$$

where 'h_{ij}' denotes the components of 'H'. Hence, when H=I (completely uncorrelated parallel sub-channels), 'ρ/N' is the signal-to-noise ratio per receive branch. Some other kinds of the normalization can also be used, where the above summation simply leads to unity.

3.4 System Model

A MIMO-OFDM system with *P* transmit antennas and *M* receive antennas is presented in Figure 3.4. To achieve a high throughput, spatial multiplexing is applied, and independent data streams are transmitted through different antennas. Before transmission, each data stream is modulated by an *N*-point IDFT, and a CP with length of L_{CP} is inserted at the beginning of each OFDM symbol. Let the i^{th} block signal from the p^{th} transmit antenna before OFDM modulation be

$$\beta_{i,p} = [\, \beta_{i,p}[0] \;\; \beta_{i,p}[1] \;\; \text{---} \;\; \beta_{i,p}[N-1]\,]^T \qquad p \in \{1, 2, \ldots, P\} \tag{3.4.1}$$

This is the *frequency-domain signal* vector [26]. Here, the frequency-domain signal is assumed to be white with zero mean and unit variance. Performing N-point IDFT, the so-called time-domain signal vector is generated as

$$b_{i,p} = [\, b_{i,p}[0] \;\; b_{i,p}[1] \;\; \text{---} \;\; b_{i,p}[N-1]\,]^T = F_N * \beta_{i,p} \tag{3.4.2}$$

Where F_N is an N x N IDFT matrix. After the CP insertion, the transmitted i^{th} OFDM symbol from the p^{th} transmit antenna is

$$s_{i,p} = [s_{i,p}[0] \; s_{i,p}[1] \;\; \text{---} \;\; s_{i,p}[N'-1]]^T \qquad N' = N + L_{CP} \tag{3.4.3}$$

$$s_{i,p}[n] = \begin{cases} b_{i,p}[n - L_{CP} + N], & 0 \le n \le L_{CP} - 1 \\ b_{i,p}[n - L_{CP}], & L_{CP} \le n \le N' - 1 \end{cases} \tag{3.4.4}$$

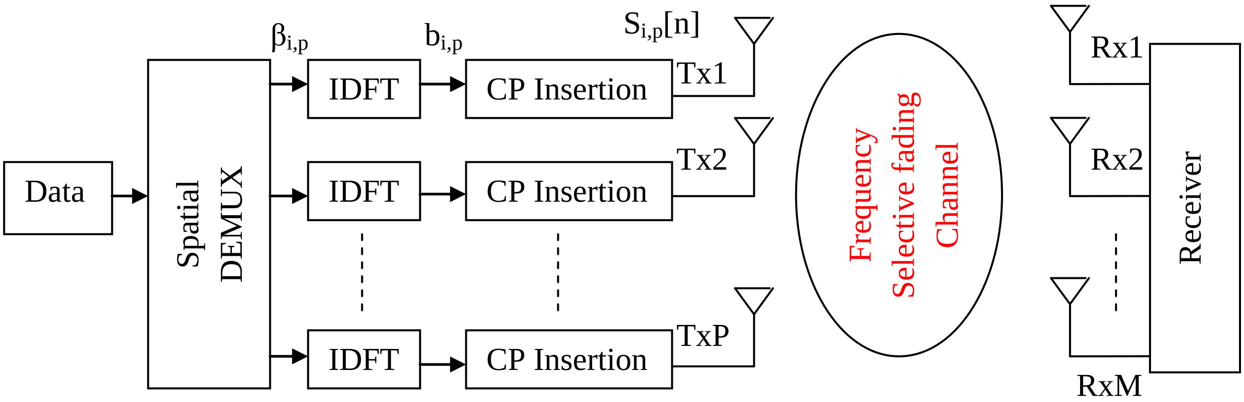

Figure 3.4: MIMO-OFDM system model

Each OFDM symbol is then simultaneously transmitted over quasi-static frequency-selective fading MIMO channels. Generally, the frequency-selective fading channel is modeled as an L-tap FIR filter, so that the M × 1 sampled received signal vector in the i^{th} received OFDM symbol is written as

$$y_i[n] = \sum_{p=1}^{P}\sum_{l=0}^{L} h_p(l) * s_{i,p}[n] + w_i[n], \qquad n = 0,1,\ldots,N' - 1. \tag{3.4.5}$$

where $h_p(l)$ is an M × 1 channel response vector; $w_i[n]$ represents the M × 1 additive noise vector; and $s_{i,p}[n] = s_{(i-1)}[N' + n]$ when $n < 0$, and $s_{i,p}[n] = s_{(i+1)}[n - N']$ when $N' \leq n$. Without loss of generality, the channel length is assumed to be far less than the number of subcarriers in one OFDM symbol, i.e., $L << N$. The noise is assumed to be independent of the transmitted signals $s_{i,p}[n]$ and is independently identically distributed complex Gaussian with zero mean and variance σ^2 [27].

Similarly to [C], the CP is not discarded, and N' *sampled* received signal vectors are collected at the receiver as

$$y_i^{(k)} = [\ y_i[-k]^T \quad y_i[-k]^T \quad \ldots \quad y_i[N'-1-k]^T\ ]^T \qquad k = 0, \pm1, \pm2, \ldots \tag{3.4.6}$$

where $\mathbf{y}_i[n]$ corresponds to the signal vector at the $(i-1)^{th}$ received OFDM symbol and is equal to $\mathbf{y}_{i-1}[n+N']$ when $n<0$, whereas it corresponds to the signal at the $(i+1)^{th}$ received OFDM symbol and is equal to $\mathbf{y}_{i+1}[n-N']$ when $N' \leq n$. In fact, the received signal vector $\mathbf{y}_i^{(k)}$ corresponds to the ith received OFDM symbol shifted by k samples and can be expressed as

$$y_i^{(k)} = H * x_i^{(k)} + w_i^{(k)} \qquad k = 0, \pm1, \pm2, \ldots \tag{3.4.7}$$

Where H, $x_i^{(k)}$ and $w_i^{(k)}$ are given in, shown at the bottom of the page. Here, the channel matrix H is assumed to be of full column rank after removing all-zero columns. This assumption is a sufficient condition to detect the time-domain signals based on the second order statistics (SOS) of the received signal vector $\mathbf{y}_i^{(k)}$[28, 29] and is generally consistent with real situations[28].

3.5 Properties of the Transmitted Signals and the Channel Matrix

The following properties of the transmitted signals and channel matrix in the MIMO-OFDM system will be used for semi-blind time domain equalization method.

Property 1: The transmitted signal $s_{i,p}[n]$ satisfies

$$E\{s_{i1,p1}[n1]*(s_{i2,p2}[n2])^H\} = \begin{cases} 1 & i1 = i2, p1 = p2 \quad (n1 = n2; |n1 - n2| = N) \\ 0 & otherwise \quad n1, n2 \in \{0,1,\ldots,N-1 \end{cases}$$

Property 2: The channel matrix H satisfies

$$H^*(H^*H^*)^\# H = \mathbf{I}_{(N'+L)P}$$

Where $\mathbf{I}_{(N'+L)P}$ is an (N'+ L)P × (N' + L)P identity matrix with all-zero rows corresponding to all-zero columns of H.

$$H = [\, H_1 \quad H_2 \quad \ldots \quad H_P \,], \qquad \text{where}$$

$$H_P = \begin{pmatrix} h_P(L) & h_P(L-1) & \cdots & h_P(0) & 0 & \cdots & 0 \\ 0 & h_P(L) & h_P(L-1) & \cdots & h_P(0) & \cdots & 0 \\ \vdots & \vdots & \vdots & \vdots & \vdots & \vdots & \vdots \\ 0 & \cdots & 0 & h_P(L) & h_P(L-1) & \cdots & h_P(0) \end{pmatrix}$$

CHAPTER- 4

SEMI - BLIND TIME DOMAIN EQUALIZER

4.1 Equalization in OFDM Systems

In general Equalization is the process of changing the frequency envelope of a sound in audio processing. Passing through any channel, an audio signal will "spread" from its original qualities. The goal of equalization is to compensate for frequency distortions in the signal. The term "equalizer" is often incorrectly applied to audio filters, such as those included on DJ mixing equipment and hi-fi audio components. However, these "equalizers" are typically general purpose audio filters, which can be arranged to produce the effect of low pass, high pass, band pass and band stop filters. Such filters are true equalizers only when arranged to *reverse* the effects of internal circuitry on sound output [30].

The issue of equalization for MIMO-OFDM systems has been widely discussed in [30, 31]. In general, there are three categories of equalization techniques.

The first one is the frequency-domain technique [30], which applies the conventional equalization algorithm for single-carrier MIMO systems to each subcarrier. Since a different equalizer is needed for each subcarrier, the design complexity is rather high, and the memory required to store the equalizer coefficients is large.

The second technique is the time–frequency domain equalization with channel shortening [29]. A time-domain equalizer is inserted to reduce the MIMO channels to the ones with the channel length shorter than or equal to the CP length, and then, a one-tap frequency-domain equalizer is applied to each subcarrier. When the MIMO channels are shortened by the time-domain equalizer, residual ICI and ISI are introduced. They cannot be eliminated by the subsequent frequency-domain equalizer and, thus, limit the performance. Moreover, it has been shown that time–frequency domain equalization techniques with channel shortening are sensitive to parameters, including the channel-shortening equalizer length and the delay.

The third technique is the time-domain statistics-based technique [32]. This method is based on some structural properties of the received OFDM symbols, which are shifted within the CP length. A time-domain equalizer, which is designed using the second-order statistics (SOS) of the shifted received OFDM symbols, is applied to partially cancel the ICI and ISI.

The equalizer output contains two sampled signals from each transmit antenna, and the time-domain signals are then detected with the aid of two pilot OFDM symbols [31].

4.2 Equalizer

Due to the channel characteristics, severe inter-symbol interference (ISI) may occur to the transmitted signals. Therefore it is necessary to use an equalizer to counter the effect of the channel. Figure 4.1 provides the system block diagram.

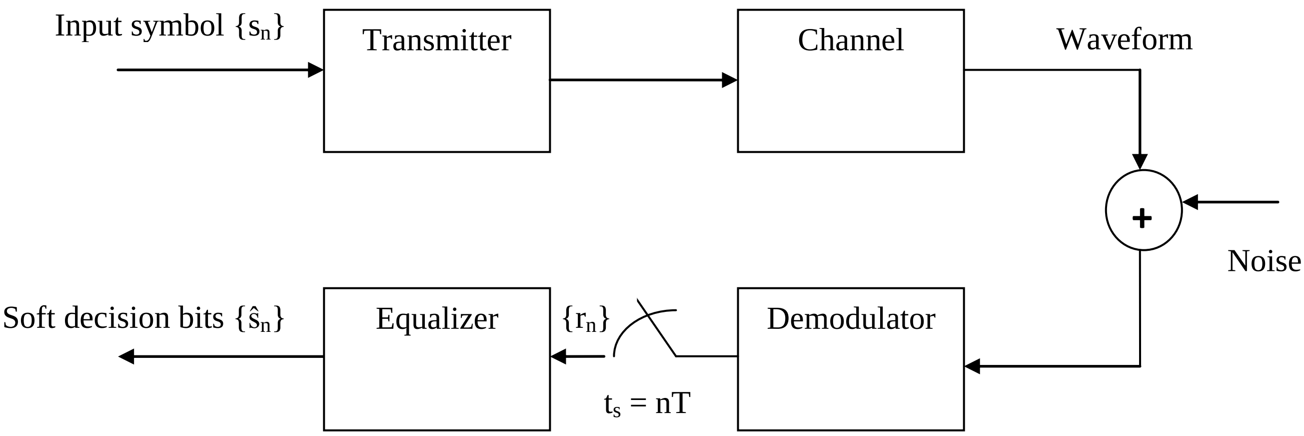

Figure 4.1: Overview of the Transmission System

In this transmission system, the input signal bits are first mapped into complex-valued symbols $\{s_n\}$, according to its modulation type. The in-phase and quadrature components of the symbol will be multiplied with the high frequency carrier and be transmitted over the additive white Gaussian noise (AWGN) channel. On the demodulator side, the received signal is demodulated with correct carrier phase into its in-phase and quadrature components, and sampled with the correct timing intervals, t_s=nT. The equalizer can be considered as a part of the demodulator. The input to the equalizer is the $\{r_n\}$ sequence, which represents the complex-valued symbols with ISI distortion, and the output is the soft decision result, which is the probability of each received bit being '1' or '0'.

There are various approaches to implement the equalizer. Basically the equalizer functions as a sequence estimator. Given the received sequence,

$$r_n = s_n + z_n$$

where s_n is the original sequence from the transmitter, and z_n is an additive white Gaussian noise process. The equalizer estimates the output sequence $\{\hat{s}_n\}$ using either hard decision or soft decision.

4.2.1 Soft Decision Bits

The aim of an Equalizer is to estimate the transmitted symbols at the receiver stage, which is more specifically to decide each bit in the symbol being a ‘0’ or ‘1’. A decision formed in a binary way of either '0' or '1' is called a hard decision. Hard decision decoding takes a stream of bits from the 'threshold detector' stage of a receiver, where each bit is considered definitely either ‘1’ or ‘0’. For binary signaling, received pulses are sampled at time intervals t_s = nT, and the resulting voltages are compared with a single threshold. If a voltage is greater than the threshold it is considered to be definitely a '1' say regardless of how close it is to the threshold. If it is less, it is definitely a ‘0’. This is equal to making a 100% positive decision of a certain bit.

Due to the present of noise, this kind of decision will cause irreversible loss of information in receiver. The remedy for this problem is by using soft decision, which instead of deciding directly the bit being '0' or '1', gives a "probability like" measure of the bit being either '0' or '1'. Soft decision decoding requires a stream of 'soft bits' where we get not only the ‘1’ or ‘0’ decision but also an indication of how certain we are that the decision is correct. The soft decision for a bit sequence [1 1 0 0] could be [20 50 -10 -90], meaning that the first two bits are probably two 1's, with the second bit more likely to be ‘1’ than the first bit, and the last two bits probably 0's, while the last bit much more likely to be ‘0’ than the third bit.

4.3 Equalization Techniques

In wireless transmission the length of the impulse response increases with propagation distances. Thus, if the guard interval/cyclic prefix (CP) is fixed to a maximum length, the channel length has to be restricted to a maximum which results in applications over short distances only (for example, ADSL) [33]. Increasing the guard interval for a fixed block length M reduces the channel throughput, since the guard interval contains redundant samples only. If we increase the block length by the same amount as the guard interval, in order to maintain reasonable bandwidth efficiency, this also increases the latency time. Note that the latency time is proportional to $M + L$, where L denotes the size of the guard interval. The presence of parallel to serial (P/S) and serial to parallel (S/P) converters as shown in Figure 2.6 makes it a crucial parameter in many applications. In order to limit the system latency time while keeping the bandwidth efficiency high, transmission with a smaller guard interval is desired. This has resulted in new receiver concepts using different equalization techniques. These techniques are briefly explained below.

4.3.1 Time-domain equalizer (TEQ)

The time domain equalization (TEQ) is a short FIR filter at the receiver input that is designed to shorten the duration of the channel impulse response (L). Thus it allows a reduction in the guard interval length [33]. Using a filter with up to 20 coefficients, the effective channel impulse response of a typical AWGN channel can easily be reduced by a factor of 10. Different cost functions such as minimum mean squared error [27], maximum shortening signal-to-noise ratio (SNR) [29], minimum inter-symbol interference (ISI) [34], and maximum bitrate [34] have been proposed to design the time domain equalizer (TEQ). An overview of the different methods and their performances is presented in [34]. Only the maximum bitrate method is optimal in terms of achievable bitrate, but its high computational complexity is prohibitive for a practical implementation.

4.3.2 Per-tone equalization

In per-tone equalization [35], the TEQ is transferred to the frequency domain, resulting in a complex frequency domain equalizer for each tone. This allows optimizing the SNR and therewith the bitrate for each tone individually. Furthermore, the equalization effort can be concentrated on the most affected tones by increasing the number of equalization filter coefficients for these tones. No effort is wasted to equalize unused subcarriers when setting the number of taps for their equalizers to zero. However, the computational complexity of the algorithm is still relatively high.

4.3.3 Multiple-input multiple-output (MIMO) equalization

The MIMO equalizer replaces the one-tap equalizer in the DMT receiver or the sequence of CP removal, DFT, and one-tap equalizer by a MIMO FIR or IIR filter [36]. Depending on the cost function applied to optimize the MIMO equalizer, we can distinguish between zero-forcing (ZF) equalization and minimum mean squared error (MMSE) equalization. ZF equalizers totally eliminate ISI and intercarrier interference (ICI), while MMSE equalizers also include additive channel noise in the cost function. It has been shown in [36] that ISI and ICI can be completely removed if the guard interval is at least equal to the length $L = 1$ and if the $M+L$ poly phase components of the channel impulse response do not have common zeros. A sufficient condition is given for the length of the FIR equalizers, which decreases with an increase of the guard interval L. Perfect equalization is even possible for common zeros of the channel poly phase components if redundancy is not introduced in terms of a cyclic prefix but as a trailing block of zeros [37].

4.3.4 Adaptive signal processing

In [38], it is proposed to replace the fixed size fast Fourier transform (FFT) in the receiver by a variable length window. A part of the received signal and the ISI is discarded. ICI due to lost orthogonality of the new windowing technique is then removed in a matched filter multistage ICI canceller.

4.4 Blind Equalization

Blind equalization algorithm designs the so-called *blind equalizer* with only the data. Unlike the Non-blind equalizers, Training data or pilot sequences are not provided for communication systems, giving the benefit of resource savings. The equalizer is usually obtained according to some statistical criteria of the data. Semi-blind Equalizers comprises a weighted mixture of the designs of the non-blind equalization and blind equalization when the amount of training or pilot source signals is not sufficient for obtaining a non-blind equalizer with acceptable performance.

Blind equalization, at first thought, seems to be unreachable because both the source signals **u**[n] and the system **H**[n] are unknown. Moreover, some potential ambiguities exist. For instance, channel output measurements **y**[n] are invariant to the pair (**H**[n]***U**, $\mathbf{U}^{-1}$***u**[n]) for any nonsingular K×K matrix **U** [39]. This implies that there must be some assumptions about the source signals **u**[n], such as temporally correlated or independent and spatially independent, and Gaussian or non Gaussian sources; and some conditions about the system **H**[n], such as full rank matrix, must possess a certain parametric form and non negativity for all the coefficients of the system. These are essential in designing the physical system for data measuring or sensing so that the unknown source signals **u**[n] can be extracted uniquely to some degree from measurements **y**[n].

Definitely, the more the source features and system characteristics are taken into account, the more accurate the extracted source signals in general. In fact many a great algorithm has been successful in blind equalization by exploitation of the properties of the source signals such as their statistical properties, constellation properties, etc. Representatives exploiting the statistical properties include maximum-likelihood (ML) algorithms, second-order statistics (SOS) based algorithms, higher-order (≥3) statistics (HOS) based algorithms and second-order cyclostationary statistics based algorithms etc.

4.4.1 Problem Statement

Suppose that u[n] is the source signal of interest and is distorted by an LTI system h[n]. The system model presented here. The system block diagram is shown in Figure 4.2.

$$y(n) = x(n) + w(n) \tag{4.4.1}$$

Where $$x[n] = h[n] * u[n] = \sum_{k=-\infty}^{\infty} h(k)u(n-k) \tag{4.4.2}$$

is the noise-free signal and $w[n]$ is the additive noise accounting for measurement noise as well as physical effects not explained by x[n]. From equations (4.4.1) and (4.4.2), it follows that

$$y[n] = h[0]u[n] + \underbrace{\sum_{k=-\infty, k\neq 0}^{\infty} h[k]u[n-k]}_{\text{ISI term}} + w[n] \tag{4.4.3}$$

From equation (4.4.3), it can be seen that the desired sample (or symbol) $u[n]$, which is scaled by a coefficient $h[0]$ in the first term is not only corrupted by the noise $w[n]$ but also interfered by other samples (or symbols) in the second term. This latter effect is called inter-symbol interference (ISI) [32].

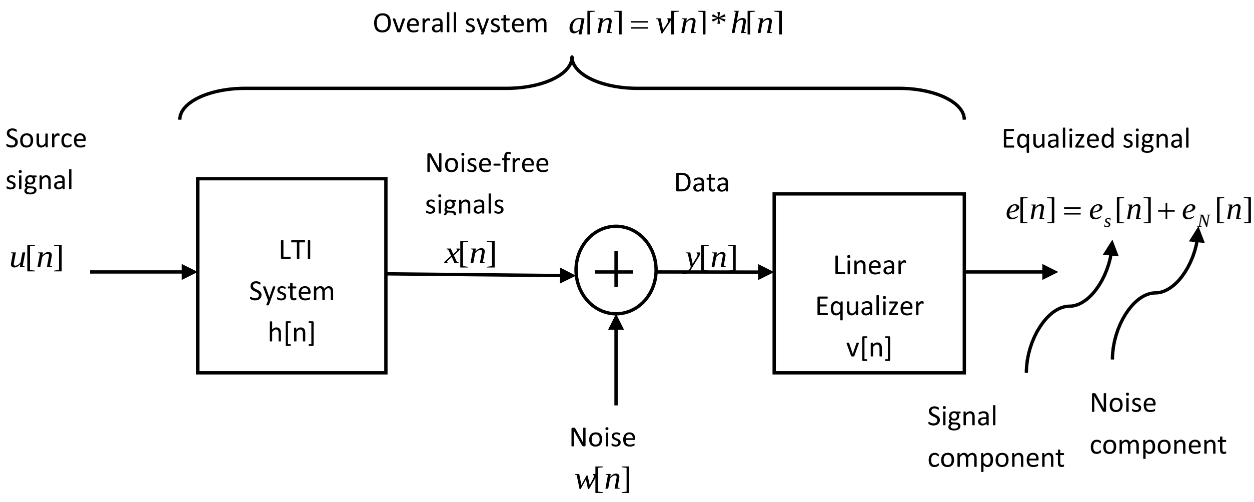

Figure 4.2: Block diagram of LTI equalization

Blind equalization, also known as "blind de-convolution", of the LTI system $h[n]$ is a signal processing procedure to restore the source signal $u[n]$ with only the data $y[n]$ generated from equations (4.4.1) and (4.4.2). This problem arises in a variety of engineering and science areas such as seismic exploration, digital communications, speech signal processing, ultrasonic nondestructive evaluation, underwater acoustics, radio astronomy and so on[40].

4.4.2 Linear Blind Equalization

To further explain the problem of blind equalization we consider the direct blind equalization approach as shown in Figure 4.2. The goal of the equalizer is to design an LTI filter, denoted by v[n], using some presumed features of u[n] such that the output of v[n] given by

$$e[n] = v[n] * y[n] = \sum_{k=-\infty}^{\infty} v(k) y(n-k) \tag{4.4.4}$$

, which approximates u[n]. The filter v[n] is called the *de-convolution filter* or the *equalizer*, or the *blind equalizer* to emphasize the use of the blind approach, while its output e[n] is called the de-convolved signal or the equalized signal. In practice, the equalizer v[n] is commonly assumed to be an FIR filter with v[n] = 0 outside a pre assigned domain of support $L_1 \le n \le L_2$ where L_1, L_2 are integers. As $L_1 = -\infty$ and $L_2 = +\infty$, the equalizer v[n] is said to be *doubly infinite*.

The signal-to-noise ratio (SNR) associated with the data y[n] is

$$SNR \equiv SNR\{y[n]\} = \frac{E\{|x[n]|^2\}}{E\{|w[n]|^2\}} \tag{4.4.5}$$

We assumed that u[n] and w[n] are uncorrelated random processes. When SNR = $+\infty$ i.e. the noise-free case, the goal of the direct blind equalization approach reduces to designing the equalizer v[n] such that the equalized signal becomes

$$e[n] = \alpha * u[n - \tau] \tag{4.4.6}$$

Where α is a real or complex constant and τ is an integer. Note that without any information about the sequences u[n] or h[n], the scale factor α and the time delay τ in the equation (4.4.6) cannot be identified for the following reason. Let $u^*[n] = \alpha * u[n - \tau]$ be another source signal and $h^*[n] = \alpha^{-1} h[n + \tau]$ another system. Then

$$h^*[n] * u^*[n] = \sum_{k=-\infty}^{\infty} \alpha h[k+\tau] \alpha^{-1} u[n-k-\tau] = \sum_{k=-\infty}^{\infty} h[k] u[n-k] = x[n] \tag{4.4.7}$$

Which indicates that both pairs (u[n],h[n]) and (u^*[n],h^*[n]) result in the same noise free signal x[n]. Hence, provision of information about x[n] or y[n] only is not sufficient to distinguish between them.

The equalized signal e[n] given by equation (4.4.4) can be further expressed as

$$e[n] = e_S[n] + e_N[n] \tag{4.4.8}$$

where $e_N[n] = v[n] * w[n]$ (by (4.4.1)) represents the noise component in e[n]

and $e_S[n] = v[n] * x[n] = g[n] * u[n]$ (by (4.4.1) and (4.4.2)) (4.4.9)

represents the corresponding signal component in which

$$g[n] = v[n] * h[n] \tag{4.4.10}$$

, is the overall system after equalization. From equations (4.4.8) and (4.4.9), it follows that unlike the noise-free case, the goal of the direct blind equalization approach for finite SNR is to design the equalizer v[n] such that the signal component e_S[n] approximates the source signal u[n] as well as possible (except for an unknown scale factor, an unknown time delay) while maintaining minimum enhancement of the noise component e_N[n].

On the other hand one can also resort to the indirect blind equalization approach to restore the source u[n] from the data y[n]. Its steps are as follows: (i) estimation of the channel h[n] by means of a blind system identification (BSI) algorithm, (ii) estimation (if needed), of other parameters such as the autocorrelation function of y[n] and (iii) design of a non blind equalizer with these estimated parameters for the retrieval of u[n] (the goal of blind equalization).

4.4.3 Performance Indices

From equations (4.4.8) and (4.4.9), it follows that for SNR = ∞ the equalized signal is

$$e[n] = g[\tau]u[n-\tau] + \sum_{k=-\infty, k\neq\tau}^{\infty} g[k]u[n-k] \tag{4.4.11}$$

If the overall system is $g[n] = \alpha\ \delta\ [n - \tau]$ (4.4.12)

Where α is a constant and τ is an integer, then the residual ISI term in (4.4.11) disappears and e[n] = α u [n− τ] which is exactly the objective for the noise-free case as shown in equation (4.4.6). This fact suggests that g[n] can serve to indicate the amount of residual ISI after equalization, thereby leading to the following commonly used performance index for the designed equalizer v[n]

$$ISI\{g[n]\} = ISI\{\alpha g[n-\tau]\} = \frac{\sum_{n=-\infty}^{\infty} |g[n]|^2 - \max\{|g[n]|^2\}}{\max\{|g[n]|^2\}} \quad (4.4.13)$$

Where α is any nonzero constant and τ is any integer. It is easy to see that the ISI{g[n]} = 0 if and only if g[n] = $\alpha\ \delta$ [n − τ] for all $\alpha \neq 0$ and all τ , implies that the smaller the value of ISI{g[n]}, the closer the overall system g[n] approaches a delta function.

On the other hand, to evaluate the degree of noise enhancement for the case of finite SNR, we may compare the SNR after equalization, defined as

$$SNR\{e[n]\} = \frac{E\{|e_S[n]|^2\}}{E\{|e_N[n]|^2\}} \quad \text{(See equation (4.4.8))} \quad (4.4.14)$$

with the SNR before equalization, i.e. SNR{y[n]} defined as (4.4.5). Alternatively, it may be more convenient to use the following performance index:

$$\rho\{v[n]\} \cong \frac{SNR\{e[n]\}}{SNR\{y[n]\}}$$, known as the SNR improvement or degradation ratio (4.4.15)

Note that ρ {v[n]} > 1 means SNR improvement after equalization, whereas ρ {v[n]} < 1 means SNR degradation after equalization.

4.5 MIMO Blind Equalization

Discrete-time MIMO LTI systems are basically the extension of discrete time Single-input single-output (SISO) LTI systems, but some of their basic properties and definitions are rather different. Moreover, an MIMO LTI system itself is a multi-variable LTI system for which some of its properties must be considered in the design of MIMO equalization algorithms. These properties comprise poles/zeros, normal rank of MIMO LTI etc.

4.5.1 Definitions

Consider a *K*-input *M*-output discrete-time LTI system defining the relation between K inputs $u_1[n], u_2[n], ..., u_K[n]$ and M outputs $x_1[n], x_2[n], ..., x_M[n]$.

Let $\mathbf{u}[n] = (u_1[n], u_2[n], ..., u_K[n])^T$ (4.5.1a)

And $\mathbf{x}[n] = (x_1[n], x_2[n], ..., x_M[n])^T$ (4.5.1b)

be the input and output vectors of this MIMO discrete-time LTI system, respectively. Then, for any input vector u[n], the output vector x[n] is completely determined by the discrete-time convolution model

$x[n] = H[n] * u[n] = \sum_{k=-\infty}^{\infty} H(k)u(n-k)$, Where H[n] is an *M* x *K* matrix defined as

$$H[n] = \begin{pmatrix} h_{11}[n] & h_{12}[n] & \cdots & h_{1K}[n] \\ h_{21}[n] & h_{22}[n] & \cdots & h_{2K}[n] \\ \vdots & \vdots & \ddots & \vdots \\ h_{M1}[n] & h_{M2}[n] & \cdots & h_{MK}[n] \end{pmatrix} \tag{4.5.2}$$

in which the (i, j)th element h_{ij} [n] is the impulse response of the SISO system from the j^th input $u_j[n]$ to the i^th output xi[n].

The M×K matrix sequence H[n] defined by equation (4.5.2) is also called the impulse response of the MIMO LTI system, with the number of rows equal to the number of system outputs and the number of columns equal to the number of system inputs. Specifically, let

$h_j[n] = (h_{1j}[n], h_{2j}[n], ..., h_{Mj}[n])^T$ is an M × 1 vector in the jth column of H[n], i.e.

$H[n] = (h_1[n], h_2[n], ..., h_K[n])$.

Then, the system output vector **x**[n] given by equation (4.5.1a) can also be expressed as

$$x[n] = \sum_{j=1}^{K} x_j[n] = \sum_{j=1}^{K} h_j[n] * u_j[n] = \sum_{k=-\infty}^{\infty} h_j[k] * u_j[n-k] \tag{4.5.3}$$

is the contribution from the j^th input $u_j[n]$ to the M outputs of **x**[n]. Moreover, the i^th output $x_i[n]$ of the system, from equations (4.5.1) and (4.5.2), can be seen to be

$$x_i[n] = \sum_{j=1}^{K} \sum_{k=-\infty}^{\infty} h_{ij}[k] u_j[n-k] \tag{4.5.4}$$

, which is also a mapping from all the K system inputs to the output $x_i[n]$. The properties of the MIMO LTI system can be introduced either directly from the properties of each individual SISO system h*ij* [n] or through transform-domain analysis of the impulse response H[n].

4.5.2 Blind Equalization Problem

Suppose that $u_1[n], u_2[n], ..., u_K[n]$ are the source signals of interest and distorted by an M × K system H[n] and the noise vector $[w_1[n], w_2[n], ..., w_M[n]]^T$ as shown in Figure 4.3. In general, the system input vector **u**[n] and noise vector **w**[n] are mutually independent stationary vector random processes, and therefore both the noise free output vector **x**[n] and the noisy output vector **y**[n] are stationary vector random processes as well. Then the correlation function and power spectral matrix of the noisy output vector **y**[n] is related to those of the noise-free output vector **x**[n] as follows:

$$R_y[l] = E\{y[n]y^H[n-l]\} = R_x[l] + R_w[l] \tag{4.5.4a}$$

$$S_y(\omega) = F\{R_y[l]\} = S_x(\omega) + S_w(\omega) \tag{4.5.4b}$$

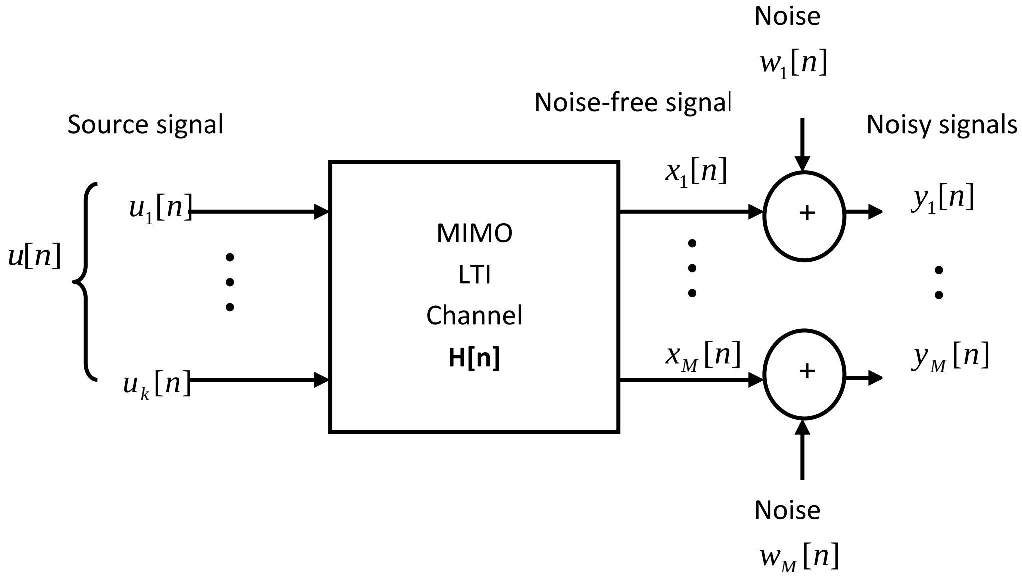

Figure 4.3: The MIMO system model

In addition to the additive noise, the system H[n] simultaneously introduces not only "temporal distortion" when H[n] ≠ Aδ[n−τ] but also "spatial distortion" when H[n] is not diagonal for all n. In wireless communications, the temporal distortion is called the inter-symbol interference (ISI) and the spatial distortion is called the multiple access interference (MAI). The blind equalization problem is to extract a desired system input $u_k[n]$ (or multiple system inputs) with a given set of measurements **y**[n] without information of the system H[n]. In other words, it is a problem to eliminate both the ISI (temporal distortion) and MAI (spatial distortion) for recovery of the desired system input $u_k[n]$ (or multiple system inputs) from the received **y**[n] without information on H[n].

4.5.3 MIMO Linear Equalization

Let **v**[n] = $(v_1[n], v_2[n], ..., v_M[n])^T$ denote a multiple-input Multiple-output (MIMO) linear equalizer to be designed as shown in Figure 4.4, that consists of a bank of linear FIR filters, with **v**[n] ≠**0** for n = L_1, L_1+1, ...,L_2 and length L = L_2-L_1+1. The equalized signal (or extracted system input) e[n] can be expressed as

$$e[n] = v^T[n] * y[n] = \sum_{j=1}^{M} v_j[n] * y_j[n] = e_S[n] + e_N[n] \tag{4.5.5}$$

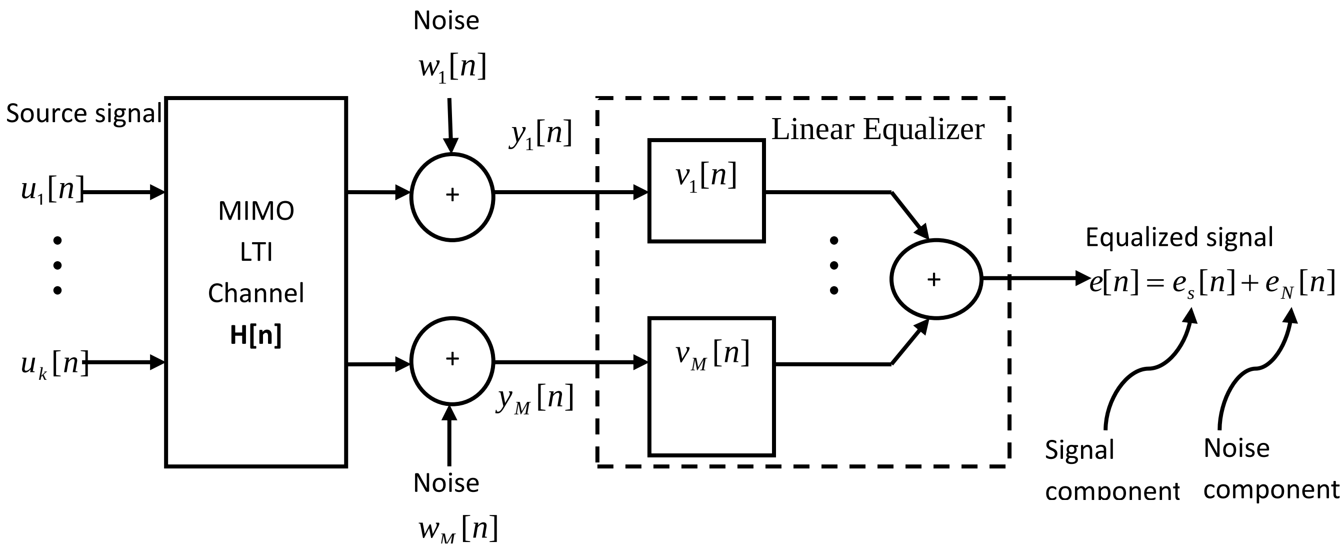

Figure 4.4: Block diagram of MIMO linear equalization

In equation (4.5.5) the term $e_N[n] = v^T[n] * w[n]$ represents the noise component and

$$e_S[n] = v^T[n] * H[n] * u[n] = g^T[n] * u[n] = \sum_{j=1}^{K} g_j[n] * u_j[n] \qquad (4.5.6)$$

is the corresponding signal component in which g[n] is the *overall system* after equalization. The signal component $e_S[n]$ given by equation (4.5.6) is depicted in Figure 4.5, in terms of the overall system g[n].

The goal of MIMO blind equalization is to design an "optimum" equalizer **v**[n] such that the signal component $e_S[n]$ approximates one input signal $u_\gamma[n]$ (up to a scale factor and a time delay) where $\gamma \in \{1, 2, ..., K\}$ is unknown. Note that the determination of γ usually needs prior information about the inputs and the associated sub-channel $h_k[n]$, depending on the application. Furthermore, all the K system inputs can be estimated through a multistage successive cancellation (MSC) procedure [30]. Finding the optimum equalizer **v**[n] is the so-called direct approach for blind equalization as introduced above. On the other hand, extraction of the desired system input (or multiple system inputs) from the received **y**[n] can also be achieved indirectly by blind system identification (also called blind channel estimation) and then by utilization of a non-blind equalizer with the use of the estimated system.

Evaluation of how an equalized signal e[n] accurately approximates the associated input $\alpha\, u_\gamma[n-\tau]$ is necessary in the MIMO equalizer design.

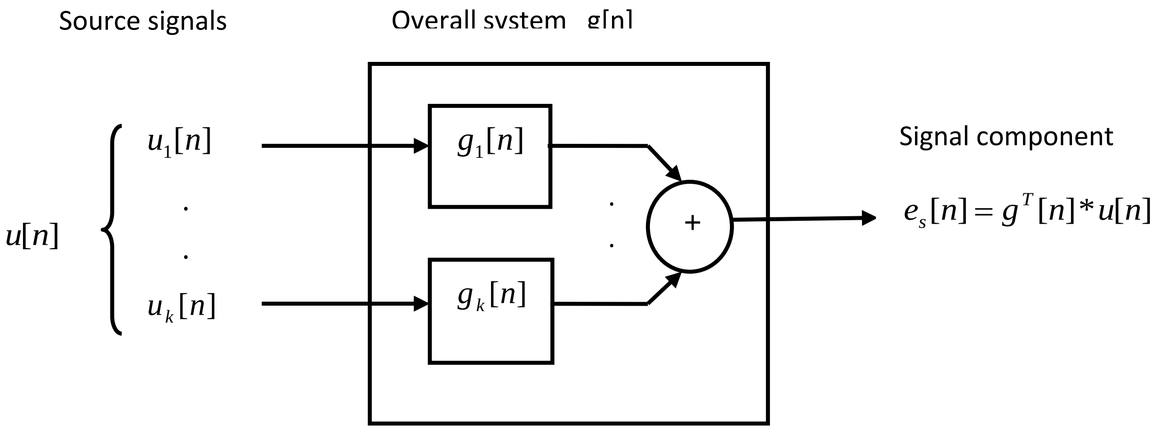

Figure 4.5: Equivalent block diagram of MIMO equalizer without noise components

4.5.4 Performance Indices

Assuming that w[n] = 0 and thus $e_N[n] = 0$, one can easily see, from equation (4.5.6), that the better the equalized signal e[n] = $e_S[n]$ approximates $\alpha\, u_\gamma[n-\tau]$, the better the resultant overall system g[n] approximates $\alpha\delta[n-\tau]\boldsymbol{\eta}$. The first commonly used performance index for the designed equalizer is the *amount of ISI* which is defined as:

$$ISI(g[n]) = \frac{\sum_{n=-\infty}^{\infty} \|g[n]\|^2 - \max_{i,n}\{|g_i[n]|^2\}}{\max_{i,n}\{|g_i[n]|^2} \geq 0 \tag{4.5.7}$$

Note that ISI($\mathbf{g}$[n]) = 0 if and only if $\mathbf{g}[n] = \alpha\delta[n-\tau]\boldsymbol{\eta}$ (for some values of α, τ). Therefore, smaller the value of ISI($\mathbf{g}$[n]), closer the overall system $\mathbf{g}$[n] to $\alpha\delta[n-\tau]\boldsymbol{\eta}$.

Another widely used performance index with noise effects taken into account is "signal-to-interference-plus-noise ratio (SINR)" of the equalized signal e[n] defined as

$$SINR(e[n]) = \frac{E\{|u_l[n]^2|\}}{E\{|e_S[n]^2|\} + E\{|e_N[n]^2|\} - \max_{k,n}\{|g_k[n]|\} * E\{|u_l[n]^2|\}} \tag{4.5.8}$$

4.6 Semi-Blind Time Domain Equalization

It is obvious from the equation (3.3.7) that the received signal vector $\mathbf{y}_i^{(k)}$ is a time-domain signal vector with multi antenna interference (MAI), ICI, and ISI. In this section, a time-domain equalization technique is proposed, as illustrated in Figure 4.6. It is a semi-blind technique since both blind information (the SOS of the received signals), and one pilot symbol will be utilized to design the equalizers.

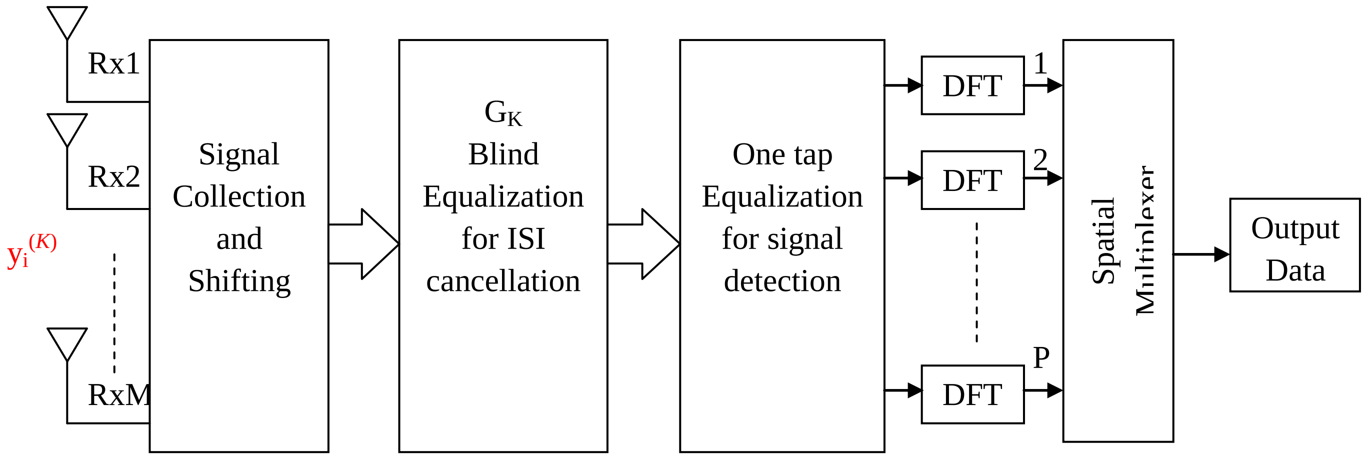

Figure 4.6: MIMO-OFDM Receiver structure

4.6.1 Blind Equalizer

Consider the autocorrelation matrices of the received signal vector $\mathbf{y}_i(k)$ in equation (3.3.7) and define,

$$R_y(0) = E\{y_i^{(Lcp)} * y_i^{(Lcp)*}\} = HE\{x_i^{(Lcp)} * x_i^{(Lcp)*}\}H^* + E\{w_i^{(Lcp)} * w_i^{(Lcp)*}\} \quad (4.6.1)$$
$$R_y(K) = E\{y_i^{(Lcp+K)} * y_i^{(Lcp)*}\} = HE\{x_i^{(Lcp+K)} * x_i^{(Lcp)*}\}H^* + E\{w_i^{(Lcp+K)} * w_i^{(Lcp)*}\} \quad (4.6.2)$$
$$R_y(-K) = E\{y_i^{(Lcp)} * y_i^{(Lcp+K)*}\} = HE\{x_i^{(Lcp)} * x_i^{(Lcp+K)*}\}H^* + E\{w_i^{(Lcp)} * w_i^{(Lcp+K)*}\} \quad (4.6.2)$$

Unlike the time-domain statistics-based technique, which considers the auto-correlation matrices (ACF) of $y_i^{(0)}$ and $y_i^{(1)}$, and the ACF matrices of $y_i^{(L)}$ and $y_i^{(LCP+K)}$ are utilized here. It is apparent that $y_i^{(L_{CP})}$ and $y_i^{(L_{CP}+K)}$, respectively, correspond to the i^{th} received OFDM symbol shifted by L_{CP} and $L_{CP}+K$ samples. It follows that $R_y(0)$, $R_y(K)$, and $R_y(-K)$ are the autocorrelation matrices of the received OFDM symbols shifted by *more than or equal to the CP length*. Here, the parameter K represents the number of shifts in excess of the CP length. Based on Property 3.4.1 the signal vectors $x_i^{(Lcp)}$ and $x_i^{(Lcp+K)}$ in equations (4.6.1)–(4.6.3) satisfy

$$E\{x_i^{(Lcp)} * x_i^{(Lcp)*}\} = \boldsymbol{I}_{(N'+L)P} \quad (4.6.4a)$$

$$E\{x_i^{(Lcp+K)} * x_i^{(Lcp)*}\} = \boldsymbol{I}_P \otimes \mathbf{J}^K \quad (4.6.4b)$$

$$E\{x_i^{(Lcp)} * x_i^{(Lcp+K)*}\} = \boldsymbol{I}_P \otimes \mathbf{J}^{-K} \quad (4.6.4c)$$

Where $\mathbf{J}^K$ denotes an $(N' + L) \times (N' + L)$ matrix with zero entries except along the lower K^{th} sub diagonal, in which the entries are '1'; $\mathbf{J}^{-K}$ is equal to $(\mathbf{J}^K)^*$. According to the definition of the matrix $\mathbf{J}^K$, the matrix $\mathbf{J}^K * \mathbf{J}^{-K}$ is equivalent to an identity matrix $\boldsymbol{I}_{(N'+L)}$ with only the first (N'+L-K) elements of the diagonal being '1'. Applying the equations (4.6.4a)-(4.6.4c) in (4.6.1)-(4.6.3) and with the assumption on the noise vector $\mathbf{w}_i^{(k)}$, it follows that

$$R_y(0) = HH^* + \sigma^2 \boldsymbol{I}_{MN'} \quad (4.6.5a)$$

$$R_y(K) = H(\boldsymbol{I}_P \otimes \mathbf{J}^K)H^* + \sigma^2(\boldsymbol{I}_P \otimes \hat{\mathbf{J}}^K) \quad (4.6.5b)$$

$$R_y(-K) = H(\boldsymbol{I}_P \otimes \mathbf{J}^{-K})H^* + \sigma^2(\boldsymbol{I}_P \otimes \hat{\mathbf{J}}^{-K}) \quad (4.6.5c)$$

where $\hat{\mathbf{J}}^K$ is an $N' \times N'$ matrix with the same structure as the matrix $\mathbf{J}^K$. From the equations (4.6.5a)-(4.6.5c), it is observed that the noise variance σ^2 is the smallest eigen value of the matrix $R_y(0)$ [28]. Therefore, it could be estimated from $R_y(0)$, and the noise effect could be eliminated from the autocorrelation matrices in equation (4.6.5). Consequently, the autocorrelation matrices without noise contribution are

$$\acute{R}_y(0) = HH^* + \sigma^2 \boldsymbol{I}_{MN'} \quad (4.6.6a)$$

$$\acute{R}_y(K) = H(\boldsymbol{I}_P \otimes \mathbf{J}^K)H^* + \sigma^2(\boldsymbol{I}_P \otimes \hat{\mathbf{J}}^K) \quad (4.6.6b)$$

$$\acute{R}_y(-K) = H(\boldsymbol{I}_P \otimes \mathbf{J}^{-K})H^* + \sigma^2(\boldsymbol{I}_P \otimes \hat{\mathbf{J}}^{-K}) \quad (4.6.6c)$$

The structures of the autocorrelation matrices of single-carrier MIMO systems are given in [41]. On comparing those results with that obtain for MIMO-OFDM systems (in equation (4.6.6)), it is easily seen that they are similar. It follows that the equalization method based on the autocorrelation matrices for single carrier MIMO systems can be readily applied here. Using equation (4.6.6), an equalizer is thus designed for ICI and ISI cancellation as

$$G_K = U_K - U_{K+1} \quad (4.6.7)$$

Where $$U_K = \acute{R}_y(-K) * \acute{R}_y(0)^{\#} * \acute{R}_y(K) * \acute{R}_y(0)^{\#} = H(\boldsymbol{I}_P \otimes \mathbf{J}^K\mathbf{J}^{-K})\, H^*(H\, H^*)^{\#} \quad (4.6.8)$$

Applying the equalizer to the received signal vector $y_i^{(k)} = H * x_i^{(k)} + w_i^{(k)}$ and using Property (3.4.2) and equation (4.6.8), it is easy to obtain the equalizer output as

$$Y_i^{(K)} = G_K * y_i^{(k)} = \textstyle\sum_P H * s_{i,p}[N' - 1 - k - K] + \eta_i^{(k)}$$

$$= H_p^{(K)} * s_i [N' - 1 - k - K] + \eta_i^{(k)} \qquad k = 0, \pm 1, \pm 2, \ldots \quad (4.6.9)$$

where $\eta_i^{(k)} = G_K * w_i^{(k)}$ is the noise component present in the symbol, can be detected by using eigen values of the auto correlation matrices, given in equations (4.6.6a)-(4.6.6c).

Obviously, only *one sampled transmitted signal* $s_{i,p}[N'-1-k-K]$ from each transmit antenna remains at the equalizer output. It turns out that both the ICI and ISI are completely eliminated. This is in contrast with the time domain statistics-based technique in *which two sampled transmitted signals from each transmit antenna* remain as shown in the equation (4.6.10) and only partial ICI and ISI cancellation is achieved in the first step of equalization [42].

$$Y_i^{(K)} = G_K * y_i^{(k)} = H_p^{(K)} * \underbrace{s_i[k]}_{\text{ISI}} + H_p^{(N'-K)} * \underbrace{s_i[N'-k]}_{\text{ISI}} + \eta_i^{(k)} \quad k = 0, \pm 1, \pm 2, \ldots \quad (4.6.10)$$

ISI

From the derivation of the blind equalizer, it is apparent that there is no restriction between the channel length L and the CP length L_{CP}, which means that the blind equalization is applicable to general MIMO-OFDM systems, irrespective of whether the CP length is longer than, equal to, or shorter than the channel length.

4.6.2 One - Tap Equalizer

Since the channel matrix H is assumed to be of full column rank after removing all zero columns and the structure of H shows that the column H $(N'+L-K)$ is a nonzero column, the matrix $H^{(K)}$ is of full column rank. Hence, signal detection is easily achieved by

$$s_{i,p}[N'-1-k-K] \approx (H_p^{(K)})^{-1} * Y_i^{(K)} \qquad k = 0, \pm 1, \pm 2, \ldots \qquad (4.6.11)$$

Where $(H^{(K)})^{-1} = (H^{(K)'} * H^{(K)})^{-1} * H^{(K)'}$, represents the *pseudo inverse matrix* of the channel matrix [33].

Up to now, signal detection is performed in time domain. To recover the frequency domain signals $\beta_{i,p}[n]$, n=0, 1, . . .,$N-1$ (refer equation (3.3.1)), the N-point DFT must be performed to the time-domain signals $b_{i,p}[n]$, n=0, 1, . . . , $N-1$(refer equation (3.3.2)), which is equal to the detected signals ($s_{i,p}[L_{CP}]$, . . . , $s_{i,p}[N'-1]$) and is obtained from the equation (4.6.11) by setting $k = N'-1-K-L_{CP}, \ldots, -K$.

It is clear that the part of the channel matrix $H_p(K)$ needs to be estimated in the signal detection technique as explained above. From equation (4.6.9), let

$\mathbf{S}_{pilot} = [\mathbf{s}_i[L_{CP}]\ \ \mathbf{s}_i[L_{CP}+1] \cdots \mathbf{s}_i[N'-1]]$ is a pilot OFDM symbol.

$\mathbf{Y}_{pilot} = [y_i^{(N'-1-k-LCP)}\ yi^{(N'-2-k-LCP)} \cdots y_i^{(-k)}]$ is the pilot's equalized output symbol, then

$$\mathbf{Y}_{pilot} = H_p(K) * \mathbf{S}_{pilot} \qquad (4.6.12)$$

and the matrix $H_p(K)$ part can be estimated using matrix inversion method as

$$H_p(K) = \mathbf{Y}_{pilot} * (\mathbf{S}_{pilot})^* (\mathbf{S}_{pilot} * (\mathbf{S}_{pilot})^*)^{-1}$$

(4.6.13)

In general, the number of subcarriers *N* in one OFDM symbol is far greater than the number of transmit antennas *P*, and the pilot matrix $\mathbf{S}_{pilot}$ can be assumed to be of full row rank.

CHAPTER- 5

SIMULATION RESULTS

5.1 Introduction

An OFDM system was modeled using MATLAB to demonstrate the effects of system parameters. The aim of this simulation was to measure the performance of MIMO-OFDM equalization with some constraints on channel length (L), cyclic prefix length (L_{CP}), number of symbols transmitted, number of receiver antennas (*P*), and number of shifts in the received symbols and finally to observe the MIMO channel capacity as a function of SNR by varying the no. of transmitting and receiving antennas used in MIMO-OFDM configuration. These simulations are done for QPSK modulation scheme that is used in IEEE 802.11a wireless LAN standard.

5.2 Constraints on CP length

In this study, a MIMO-OFDM system with $P = 2$ transmit antennas and $M = 4$ receive antennas was considered as an example. The number of subcarriers in each OFDM symbol is $N = 32$, and the length of CP is $L_{CP} = 8$. One pilot OFDM symbol is inserted at the beginning of each data packet with N_S=500 OFDM symbols. The frequency selective fading channel responses are randomly generated with a Rayleigh probability distribution. The parameter *K* is set to 8.

The autocorrelation matrices $R_y(0)$, $R_y(K)$, and $R_y(-K)$ are computed as follows:

$$R_y(0) = E\{(y_i^{L_{CP}})^* * y_i^{L_{CP}}\} = \frac{1}{N_s}\sum_{i=1}^{N_s}(y_i^{L_{CP}})^* . y_i^{L_{CP}}$$

$$R_y(K) = E\{(y_i^{L_{CP}})^* * y_i^{K+L_{CP}}\} = \frac{1}{N_s}\sum_{i=1}^{N_s}(y_i^{L_{CP}})^* . y_i^{K+L_{CP}}$$

$$R_y(-K) = E\{y_i^{L_{CP}} * (y_i^{K+L_{CP}})^*\} = \frac{1}{N_s}\sum_{i=1}^{N_s}(y_i^{K+L_{CP}})^* . y_i^{L_{CP}}$$

5.2.1 Case with L ≤ L_{CP}

At first the channel length was made to have ‘8’ samples and CP length to ‘6’ samples. Here the effect of frequency-selective fading was eliminated by the standard OFDM technique, and the signals were recovered by a one-tap frequency domain equalizer on each subcarrier. Figure 5.1 illustrates the performance comparison of the proposed Semi-blind domain TDE technique with the conventional TDE technique. Results show that the performance of the proposed technique is close to that of the conventional technique and confirm that the blind equalizer designed in the first step can completely suppress both ICI and ISI. Figure 5.2 shows the constellation diagram of corresponding received symbols at SNR = 20dB for QPSK modulation scheme.

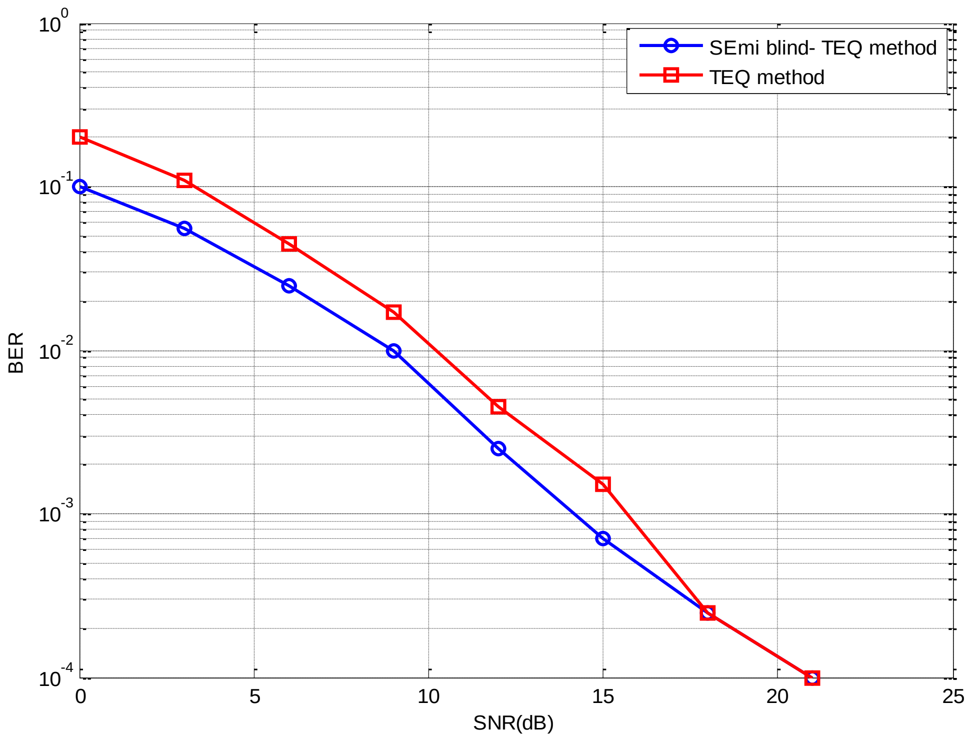

Figure 5.1: BER vs. SNR with case L $\leq L_{CP}$ (L=6)

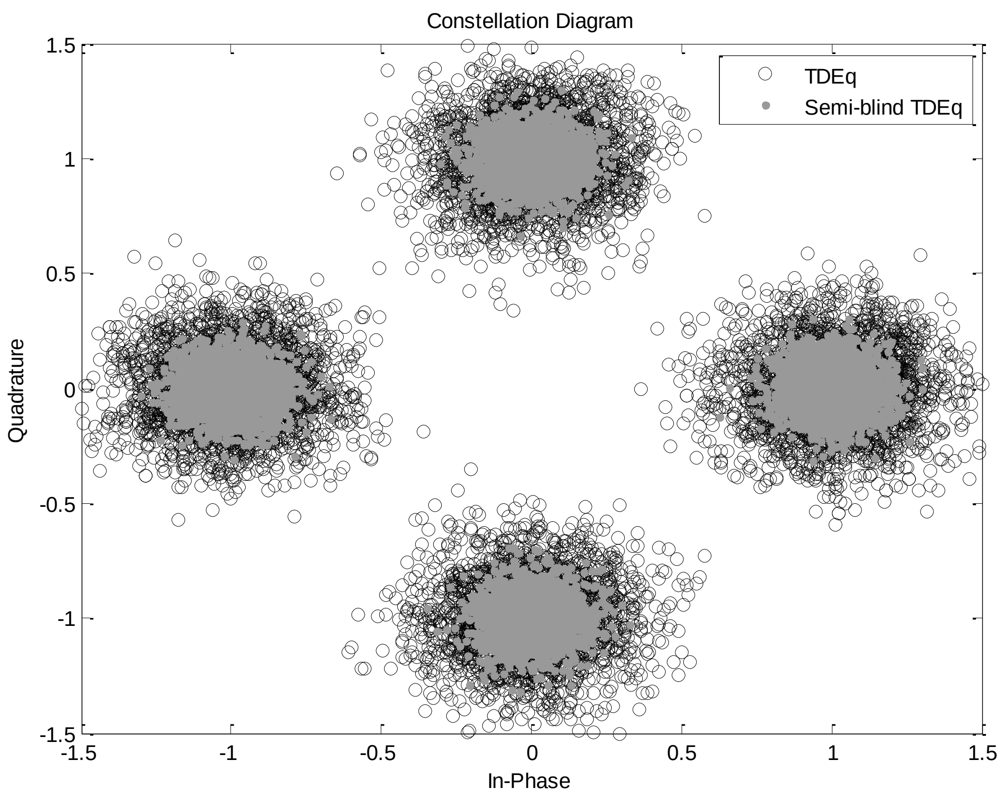

Figure 5.2: Received symbol's Constellation with case L $\leq L_{CP}$ (L=6)

5.2.1 Case with L ≥ L_{CP}

Since the channel length is longer than the CP length, the effect of frequency-selective fading cannot be completely eliminated by the standard OFDM technique, and ICI and ISI are introduced. The BER performance results of the proposed technique and the conventional technique are compared in Figure 5.3. Obviously, the Blind TEQ outperforms the conventional technique. We can observe the constellation diagram of received symbols at an SNR of 20 dB in the Figure 5.4. The performances of the two techniques are close for SNR ≤ 9 dB only. This can be explained as follows: The time domain signals are detected after ICI and ISI are eliminated by blind equalization in the proposed technique, whereas there are residual ICI and ISI in the TEQ technique. When the SNR is low, the additive noise dominates; hence, the performances of the two techniques are similar. The poorer performance of the TEQ technique is probably due to a single pilot OFDM symbol being used. Instead of a single pilot, if we use 2 or more pilot symbols, the BER performance may improve and hence the effect of ICI and ISI also may reduce drastically.

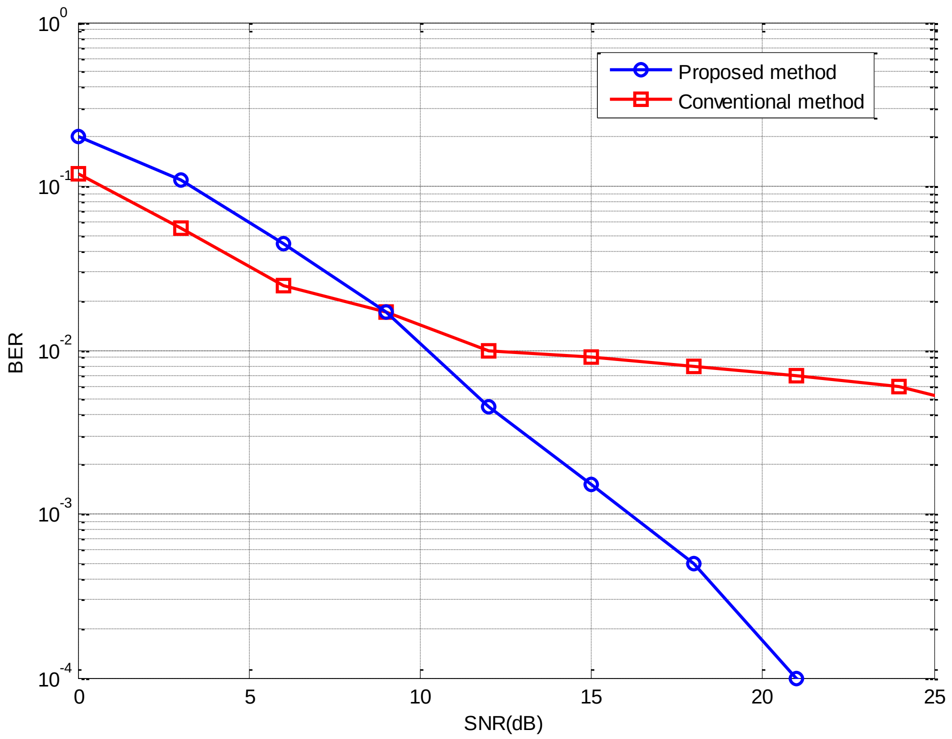

Figure 5.3: BER vs. SNR with case L ≥ L_{CP} (L=10)

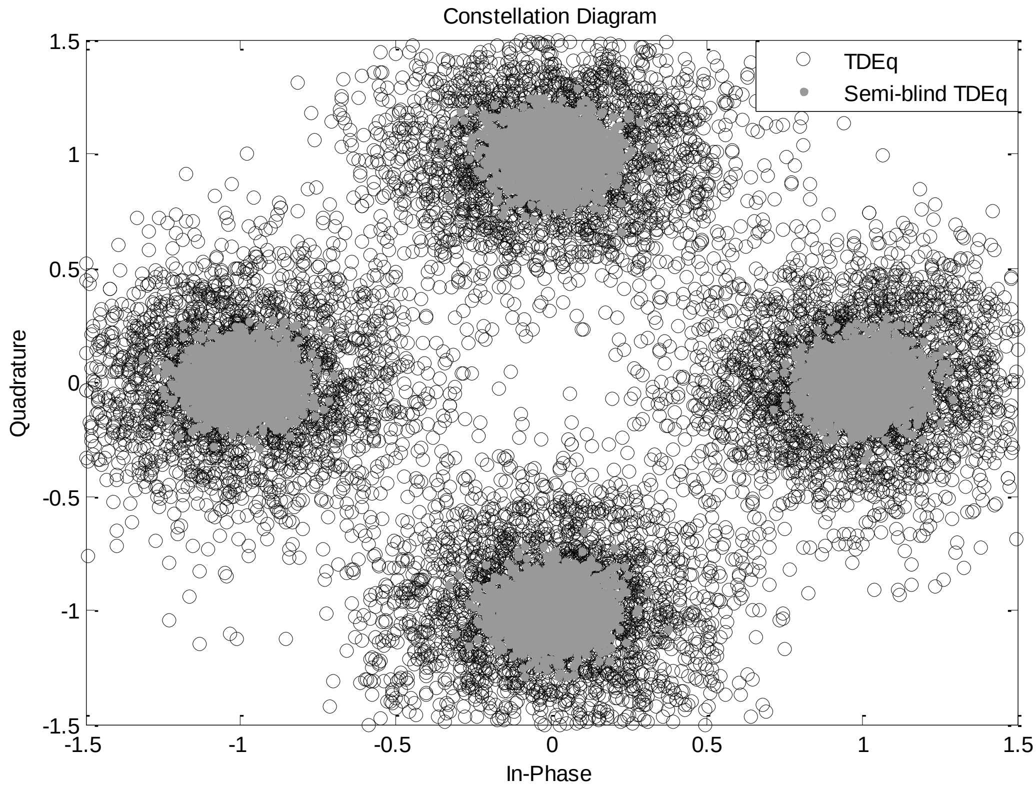

Figure 5.4: Received symbol's Constellation with case L ≥ L_{CP} (L=10)

5.3 Effect of the parameter K

All the system parameters in the proposed technique were kept constant except the no. of shifts in excess of CP length in received symbols; i.e. 'K'. This is set to vary from 1 to 8 to test its effect on the proposed technique's BER performance. The simulation was carried out at SNR=15dB. Results are shown in Figure 5.5 for both the ($L \leq L_{CP}$, $L > L_{CP}$) cases. The results show that the performance of the proposed technique is insensitive to the parameter K. This is an advantage over the FEQ, TEQ and time–frequency domain techniques, which are sensitive to the channel-shortening equalizer length and the delay.

5.4 Effect of the Data Length Ns

The semi-blind equalizer in the proposed technique was designed using the autocorrelation matrices [$R_y(0)$, $R_y(K)$, and $R_y(-K)$] shown in session 5.2. In practice, they are computed from a finite number of OFDM symbols, and the number of symbols used, i.e., Ns, may affect the performance. Figure 5.6 shows the BER performance when Ns varies from 50 to 500 at a fixed SNR of 15 dB for both the ($L \leq L_{CP}$, $L > L_{CP}$) cases. The results show that better performance is achieved when more OFDM symbols are used.

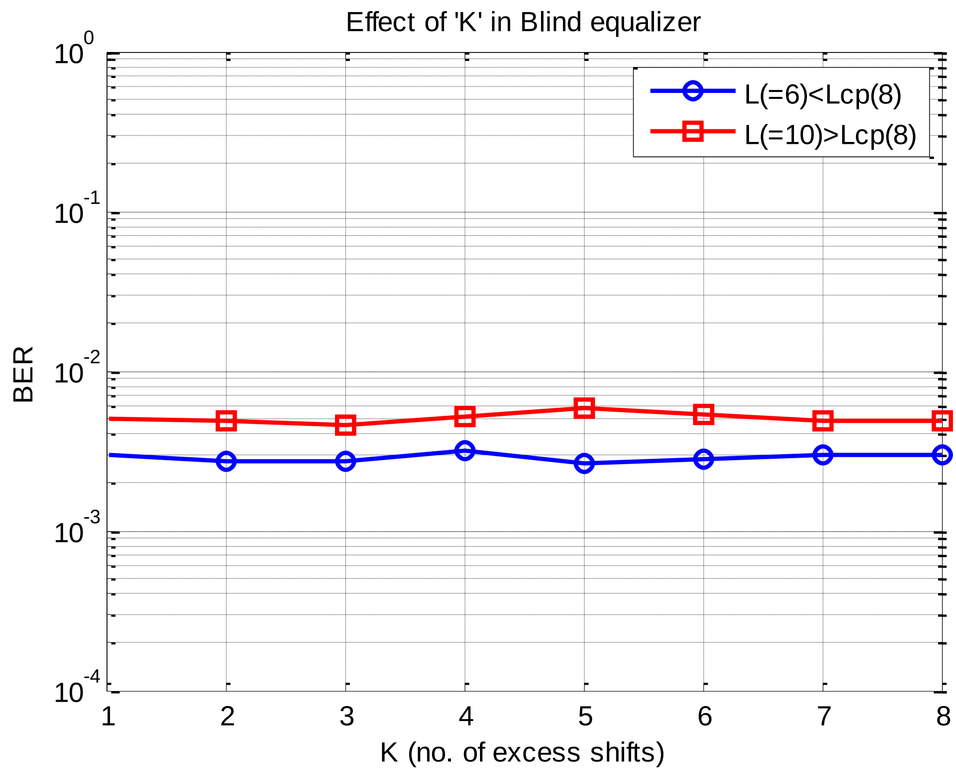

Figure 5.5: Effect of '*K*' (SNR=15dB)

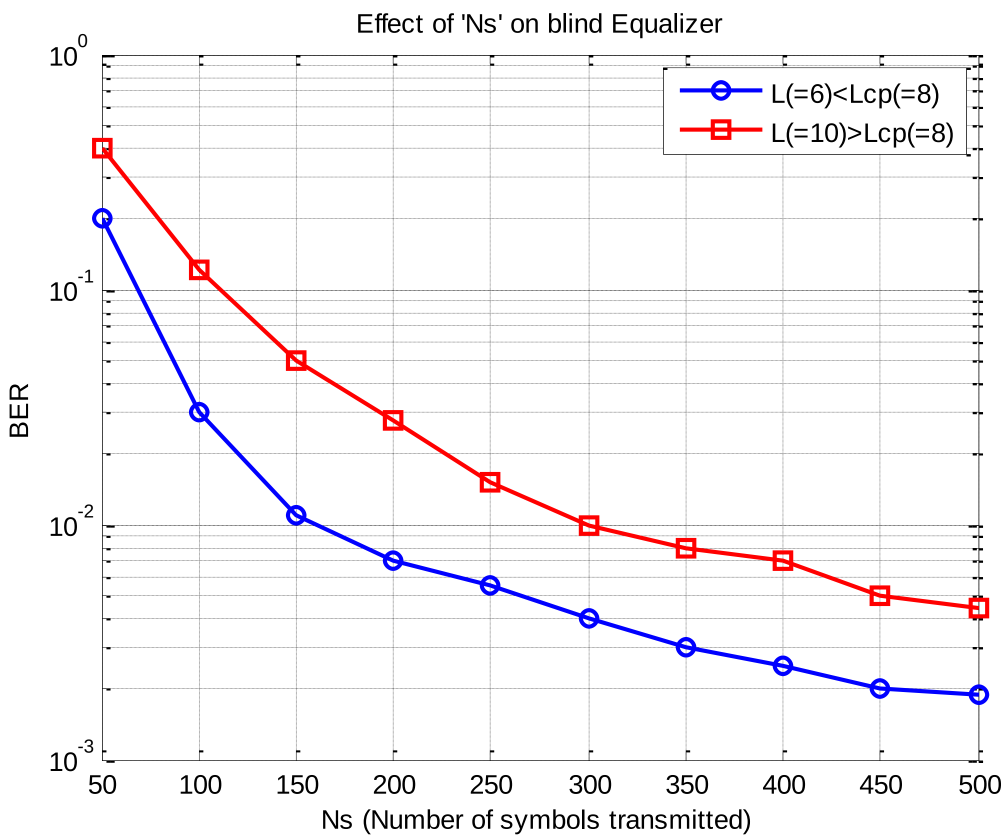

Figure 5.6: Effect of 'N_S' (SNR=15dB)

5.5 MIMO channel Capacity

A simple MIMO antenna configuration is considered with Rayleigh fading channel. The no. of transmit and receive antennas are assumed to be same. The channel matrix's size depends upon the no. of antennas used. Figure 5.7 shows the capacity of Rayleigh fading channel in bits per second (bps) for different MIMO configurations over SNR ranged from 0dB to 20dB. The bandwidth is assumed to be unity (Hz).

Figure 5.8 shows the same as a function of no. of antennas used at different SNR levels. The simulation results directly follows the "Shannon-Fanon's Channel Capacity Theorem", which states that as SNR or diversity increases, the channel capacity increases for a fixed bandwidth.

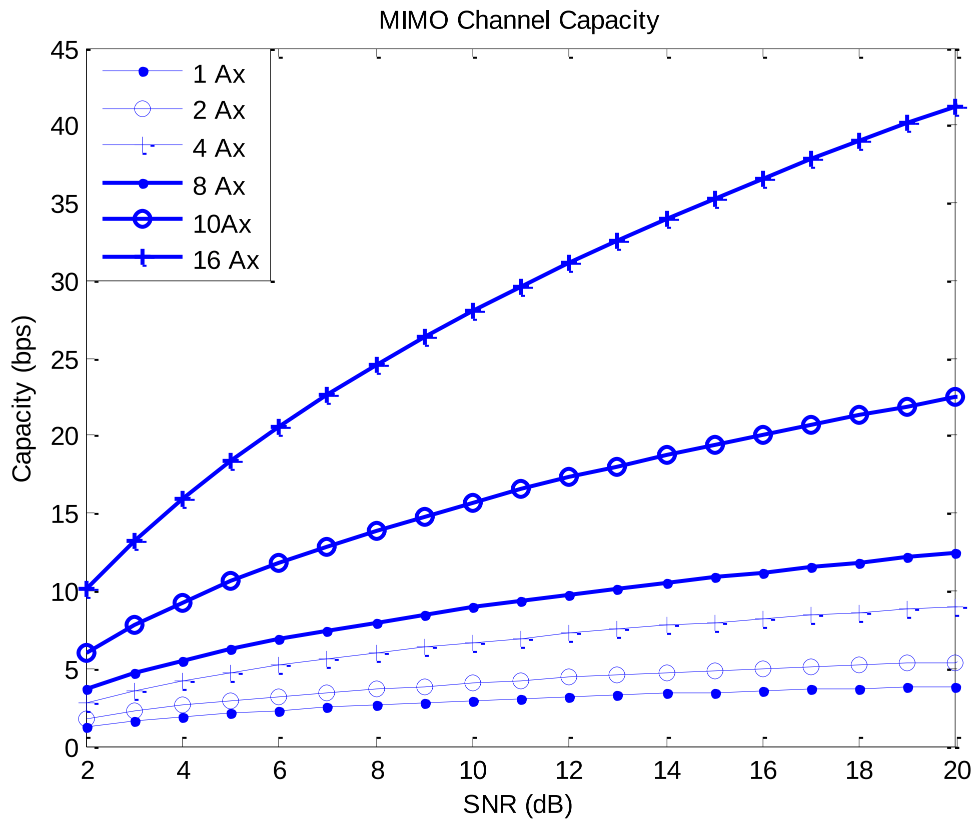

Figure 5.7: MIMO channel capacity as a function of SNR

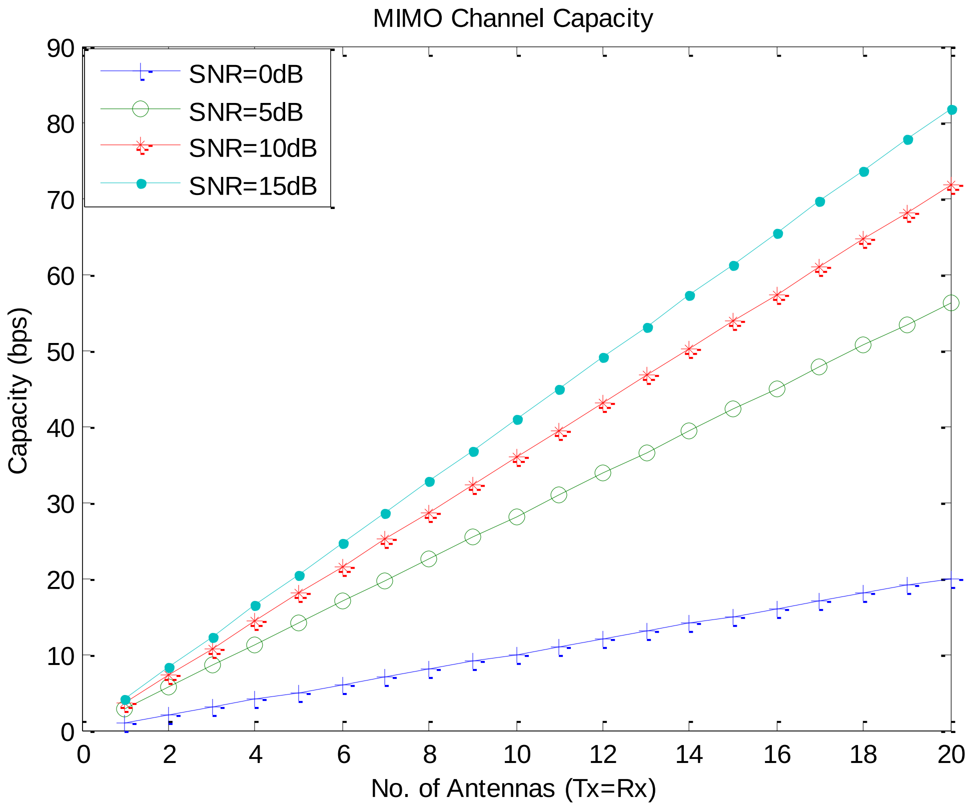

Figure 5.8: MIMO channel capacity as a function of No. of Antennas used.

5.6 Computation Burden of System

Computation of DFT and IDFT matrices require $O(N^2)$ multiplications. The channel matrix is of the order P*(2L+1) x (L+1). Hence the convolution with OFDM symbols requires $O(N^3)$ multiplications and $O(N^2)$ additions. Auto Correlation matrices also require nearly same no. of calculations.

CONCLUSION

In this thesis, a semi-blind time-domain equalization technique has been proposed for general MIMO-OFDM systems. It performs well irrespective of whether the CP length is longer than, equal to or shorter than the channel length. The added CP at the end of each MIMO-OFDM symbol converts the *linear convolution* in the channel into *circular convolution.* This process results in DFT upon transforming into frequency domain. Hence, we can fully depend upon the DFT / IDFT blocks used in MIMO OFDM transmission block diagram without any constraints on them. The blind equalizer has been designed using the SOS of the received OFDM symbols *shifted by more than or equal to the CP length* to completely suppress both ICI and ISI. The time-domain signals are then detected from the blind equalizer output with the aid of only one pilot OFDM symbol. Simulations have demonstrated that the proposed semi-blind time domain equalizer technique is effective in suppressing ICI and ISI and robust against the number of shifts in excess of the CP length.

FUTURE SCOPE

In this thesis, the main concentration in simulation was on the length of CP inserted at the end of each MIMO-OFDM symbols, which is an unwanted overhead. Even though this added CP creates a *circular convolution* in the multi-path channel, it increases the power to be transmitted unnecessarily. Instead of inserting the part of a symbol at its tail, it is advisable to insert zeros, which is known as *zero padding* (ZP) a recent technique. The whole simulation work done in this thesis can be tested for ZP instead of CP. It is also advisable to observe the effect of the total frame length on the performance of the proposed equalizer. This proposed equalizer can be implemented to Wi-max (IEEE 802.16) network standards.

REFERENCES

[1] A. Paulraj, D. Gore, R. Nabar, and H. Bolcskei, *"An overview of MIMO communications A key to gigabit wireless," Proc. IEEE*, vol. 92, no. 2, pp. 198–218, Feb. 2004.

[2] B. Muquet, Z. Wang, G. B. Giannakis, M. de Courville, and P. Duhamel, *"Cyclic prefixing or zero padding for wireless multicarrier transmissions?" IEEE Trans. Commun.*, vol. 50, no. 12, pp. 2136–2148, Dec. 2002.

[3] Wayne Stark, Wireless Technologies and Information Networks, Multiple-Access Techniques, http://www.wtce.org/loyola/wireless/02_04.htm.

[4] Ramjee Prasad, OFDM for Wireless Communications Systems, Artech House Universal Personal Communications series, 2004, ISBN: 978580537960.

[5] B. Salzberg, *"Performance of an efficient parallel data transmission system", IEEE Trans. Commun. Technol.*, vol. COM-15, pp. 805-813, Dec. 1967.

[6] R.W. Chang, *"Synthesis of Band-Limited Orthogonal Signals for Multichannel Data Transmission", Bell Syst. Tech. J.*, vol.45, pp. 1775-1796, Dec. 1966.

[7] J. A. C. Bingham, Multicarrier modulation for data transmission: *"An idea, whose time has come,"* IEEE Commun. Mag., vol. 28, pp. 5-14, May 1991.

[8] S.B. Weinstein, P.M. Ebert, *"Data transmission by frequency-division multiplexing using Discrete Fourier transform", IEEE Trans. Commun. Technol.*, vol. COM-19, pp. 628-634, Oct. 1971.

[9] John G.Proakis, Dimitris G.Manolakis, Digital signal processing, Principles, Algorithms, and Applications, Indianapolis: Prentice- Hall publications, 2007, ISBN: 9780133737622.

[10] Simon Haykin, Digital Communications, Singapore, Wiley Publications Ltd, 1988. ISBN: 9780471432227.

[11]Xinhua Wang, Michael Chow, Sheng-Mou Yu,*"QPSK Modulation and Demodulation,"* ELE 791 Software Radio Design, Syracuse University, Department of Electrical Engineering, Dec 14th 2004.

[12]Theodore S.Rappaport, Wireless Communications, principles and practice, 2nd Edition, Prentice- Hall publications, Oct 2001, ISBN: 978521826294.

[13]Eldo Mabiala, Mathias Coinchon, Karim Maouche, *"Study of OFDM modulation,"* Eurecom institute, December 1999.

[14]Duran Mattie, *"Introduction to OFDM, OFDM as a possible modulation technique for multimedia, applications in the range of mm waves,"* TUD-TVS, 10/30/98.

[15]Charan Langton, Analysis & Simulation Group, Loral Space Systems, Intuitive Guide to Principles of Communications, http://www.complextoreal.com/chapters/mft.pdf.

[16]Black Team, Jia Liu, Erik Bergenudd, Vinod Patmanathan, Romain Masson, OFDM Project, Final report, 2E1367 - Project Course in Signal Processing and Digital Communication, KTH, Stockholm,30th May 2005.

[17]B. Sklar, *"Rayleigh Fading Channels in Mobile Digital Communication Systems-Part I: Characterization,"* IEEE Commun. Mag., July 1997.

[18]Mosier, R. R., and Clabaugh, R.G.," *A Bandwidth Efficient Binary Transmission System," IEEE Trans., Vol. 76, pp. 723 - 728, Jan. 1958.*

[19]Charan Langton, Tutorials in Communication Engineering, Intersymbol Interference (ISI) and Raised cosine filtering, http://www.complextoreal.com/chapters/isi.pdf.

[20]W. Henkel, G. Taubock, P. Olding, *"The cyclic prefix of OFDM/DMT – an analysis,"* International Zürich Seminar on Broadband Commu. Zürich, Switzerland, February 2002.

[21]A. Paulraj, R. Nabar, D. Gore, *"Introduction to Space-Time Wireless Communications,"* Cambridge university Press, May 2003, ISBN: 978521826152.

[22]J. H.Winters, J. Salz, and R. D. Gitlin, *"The impact of antenna diversity on the capacity of wireless communication systems,"* *IEEE Trans. Commun.*, vol. 42, no. 2–4, pp. 1740–1751, Feb.–Apr. 1994.

[23]G. G. Rayleigh and J. M. Gioffi, "Spatio-temporal coding for wireless communications," *IEEE Trans. Commun.*, vol. 46, pp. 357–366, Mar. 1998.

[24]D. S. Shiu *et al.*, "Fading correlation and its effect on the capacity of multi element antenna systems," *IEEE Trans. Commun.*, vol. 48, pp. 502–513, Mar. 2000.

[25]G. J. Foschini and M. J. Gans, "On limits of wireless communications in a fading environment when using multiple antennas," *Wireless Personal Commun.*, vol. 6, no. 3, pp. 311–335, Mar. 1998.

[26]S. Ma and T. S. Ng*"Semi-Blind Time-Domain Equalization for MIMO-OFDM Systems," IEEE Trans. Vehicular Technology*., vol. 57, no. 4, pp. 2219-2227 Jul, 2008.

[27]Heidi Steendam, Marc Moeneclaey, *"Optimization of OFDM on Frequency-Selective Time Selective Fading Channels," IEEE Trans. Signal Processing*, vol. 32, no. 10, pp. 1431–1441, Sep. 1998.

[28]Y. Zeng and T. S. Ng, *"A semi-blind channel estimation method for multiuser multi antenna OFDM systems," IEEE Trans. Signal Process.* vol. 52, no. 5, pp. 1419–1429, May 2004.

[29]A. Gorokhov, P. Loubaton, *"Subspace-based techniques for blind separation of convolutive mixtures with temporally correlated sources," IEEE Trans. Circuits Syst. Fundam. Theory Appl.*, vol. 44, no. 9, pp. 813–820, Sep. 1997.

[30]Johnny Nelson, "*Real time Digital Signal Processing - 3 Band Graphic Equalization with Bass and Treble Shelving and Gain Control*" University of North Texas, EENG 3910 - Project V - DSP System Design, Course webpage – Fall 2007.

[31]P. J. W. Melsa, R. C. Younce, and C. E. Rohrs, *"Impulse response shortening for discrete multitone transceivers," IEEE Trans. Commun.*, vol. 44, no. 12, pp. 1662–1672, Dec. 1996.

[32]G. Leus and M. Moonen, "*Per-tone equalization for MIMO OFDM systems," IEEE Trans. Signal Process.* vol. 51, no. 11, pp. 2965–2975, Nov. 2003.

[33]M. Nafie, A. Gatherer, *"Time-domain equalizer training for ADSL," IEEE International Conference on Communications*, vol. 2, pp. 1085–1089, Montreal, Quebec, Canada, June 1997.

[34]G. Arslan, B. L. Evans, and S. Kiaei, *"Equalization for discrete multitone transceivers to maximize bit rate," IEEE Trans. Signal Processing*, vol. 49, no. 12, pp. 3123–3135, 2001.

[35]K. Van Acker, G. Leus, M.Moonen, O. van deWiel, and T. Pollet, *"Per tone equalization for DMT-based systems," IEEE Trans. Communications*, vol. 49, no. 1, pp. 109–119, 2001.

[36]X.-G. Xia, *"New precoding for intersymbol interference cancellation using non-maximally decimated multirate filterbanks with ideal FIR equalizers," IEEE Trans. Signal Processing*, vol. 45, no. 10, pp. 2431–2441, Sep. 1997.

[37]P. P. Vaidyanathan, Multirate Systems and Filter Banks, Englewood Cliffs, NJ, USA, Prentice Hall, 1993, ISBN: 9780136057185.

[38]N. Suzuki, H. Uehara, and M. Yokoyama, *"A new OFDM demodulation method to reduce influence of ISI due to longer delay than guard interval,"* in *Proc. 8th IEEE International Conference on Communication Systems*, vol. 1, pp. 239–244, Singapore, November 2002.

[39]Chong Y. Chi, Blind Equalization and System Identification, London: Springer series, British Library Cataloguing in Publication Data, 2006, ISBN: 9781846280221.

[40]J K. Tugnait, *"Identification and deconvolution of multichannel linear non Gaussian processes using higher-order statistics and inverse filter criteria,"* IEEE Trans. Signal Processing, vol. 45, no. 3, pp. 658–672, Mar. 1997.

[41]J. Zhu, Z. Ding, and X. R. Cao, *"Column-anchored zero-forcing blind equalization for multiuser wireless FIR channels," IEEE J. Sel. Areas Commun.*, vol. 17, no. 3, pp. 411–423, Mar. 1999.

[42]S. D. Ma and T. S. Ng, "Time domain signal detection based on second order statistics for MIMO-OFDM systems," *IEEE Trans. Signal Process.* vol. 55, no. 3, pp. 1150–1158, Mar. 2007.